



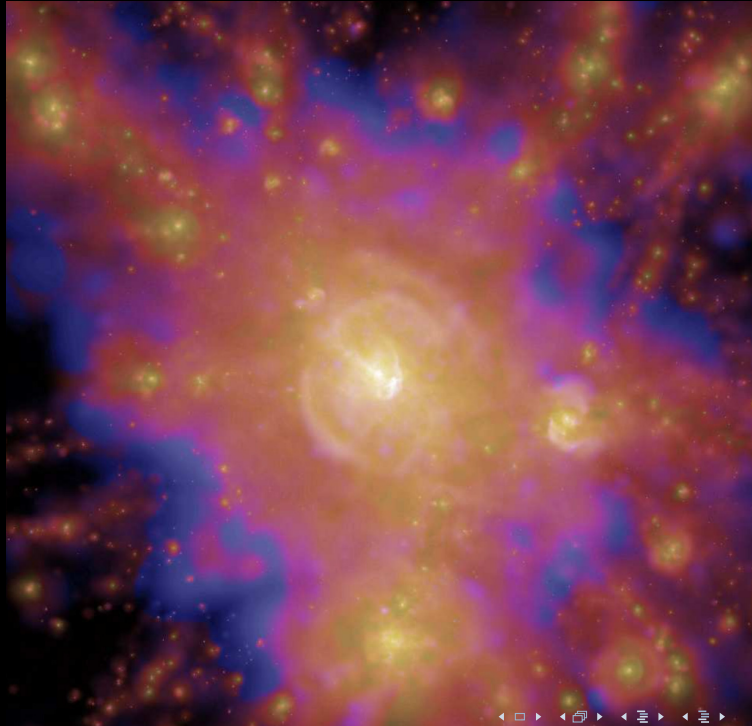
The Physics of Galaxy Clusters
15th Lecture

Christoph Pfrommer

Leibniz Institute for Astrophysics, Potsdam (AIP)

University of Potsdam

*Lectures in the International Astrophysics
Masters Program at Potsdam University*



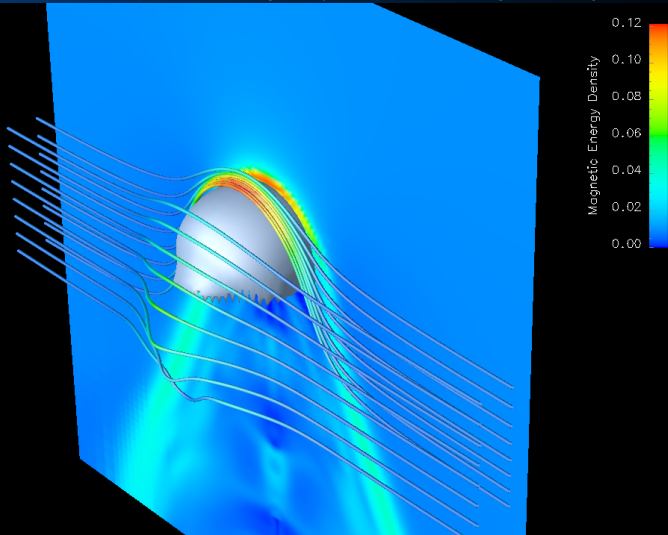
Outline

- 1 Magnetic draping
 - Physics
 - Analytics
 - Simulations
- 2 Cluster radio emission
 - Shocks and radiative processes
 - Radio relic phenomena
 - Radio halos
- 3 Galaxy cluster cosmology



What is magnetic draping?

Interaction of an obstacle (Earth, star, galaxy, ...) with a magnetized plasma



What is magnetic draping?

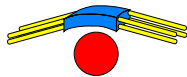
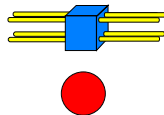
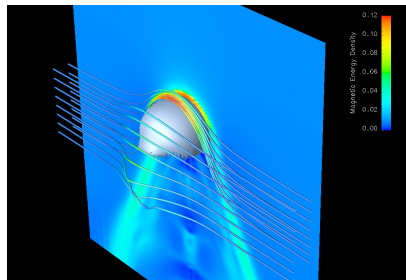
Interaction of a moving object (star, galaxy, ...) with a magnetized plasma

Consider the rest frame of the object:

- **magnetic flux is frozen into the plasma** that is advected onto the object
- **competition between “plowing up” and slipping around** of field lines set field strength in draping layer:

$$\frac{B^2}{8\pi} = \alpha \rho_0 v^2$$

- **magnetic pressure** pushes field lines around the object
- **magnetic tension and inertia of the flux-frozen magnetic field** that is anchored and advected with the ambient plasma **slow down object**



Thickness of the draping sheath - analytics

Energy density of magnetic draping sheath balances ram pressure:

$$B = \frac{B_0}{\sqrt{1 - \frac{R^3}{(R+s)^3}}} \approx \sqrt{\frac{R}{3s}} B_0 + \mathcal{O}\left(\sqrt{\frac{s}{R}}\right)$$

$$P_B = \frac{B^2}{8\pi} = P_{B_0} \frac{R}{3s} = \alpha \rho_0 v^2$$

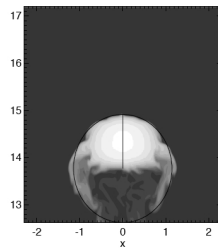
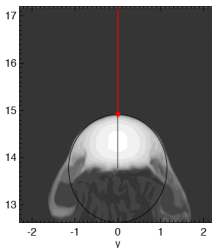
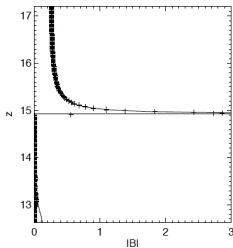
$$\mathcal{M}_A^2 = \frac{v^2}{v_A^2} = \frac{\rho_0 v^2}{2P_{B_0}} = \frac{1}{2} \beta \gamma \mathcal{M}^2$$

$$l_{\text{drape}} \equiv s = \frac{R}{6\alpha \mathcal{M}_A^2} = \frac{R}{3\alpha \beta \gamma \mathcal{M}^2} \sim 100 \text{ pc},$$

for $R \simeq 30 \text{ kpc}$, $\beta = P_{\text{th}}/P_B \simeq 50$, and a trans-sonic flow, $\mathcal{M}^2 \simeq 1/\gamma$.



Thickness of the draping sheath – simulations



amplified draping field $B = \frac{1}{\sqrt{1 - \frac{R^3}{r^3}}} B_0$, $l_{\text{drape}} \simeq \frac{R}{6\alpha M_A^2}$ with $\alpha \simeq 2$;

left: fitting peak position and a fall-off radius of the theory prediction;
right: density cut-planes; circle shows radius and position given by the fit to the magnetic field structure, left;

→ astonishing agreement of curvature radius at the working surface with potential flow predictions!

Magnetic energy of the draping layer

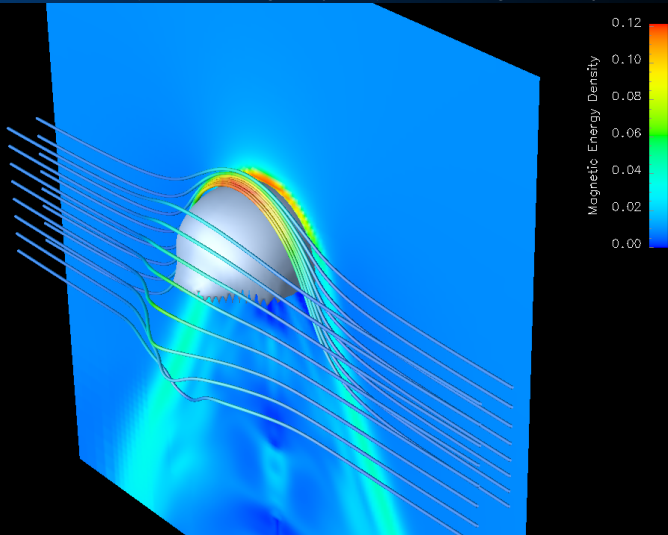
- in the draping layer, $\varepsilon_B \simeq \alpha \rho v^2$, is solely given by the ram pressure and *completely* independent of ε_{icm}
- assume sphere with radius R and volume V_{sph} , constant thickness of the drape l_{drape} over an area $A = 2\pi R^2$:

$$\begin{aligned}
 E_{B, \text{drape}} &= \frac{B_{\text{drape}}^2}{8\pi} A l_{\text{drape}} = \frac{B_{\text{drape}}^2}{8\pi} \frac{A R}{6\alpha \mathcal{M}_A^2} \\
 &= \alpha \rho v_{\text{gal}}^2 \frac{A R}{6\alpha} \frac{B_{\text{icm}}^2}{4\pi \rho v_{\text{gal}}^2} = \frac{1}{2} \varepsilon_{B, \text{icm}} V_{\text{sph}} = \frac{1}{2} E_{B, \text{icm}}
 \end{aligned}$$

→ “Archimedes principle of magnetic draping”

What is magnetic draping?

Interaction of an obstacle (Earth, star, galaxy, ...) with a magnetized plasma



Energetics of cluster mergers

- **Galaxy cluster mergers** dissipate a gravitational binding energy of

$$E_{\text{pot}} \simeq \frac{3}{5} \frac{GM_{\text{cl}}^2}{r_{\text{cl}}} \simeq 2.6 \times 10^{64} \text{ erg} \left(\frac{M_{\text{cl}}}{10^{15} M_{\odot}} \right)^2 \left(\frac{r_{\text{cl}}}{2 \text{ Mpc}} \right)^{-1}$$



Energetics of cluster mergers

- **Galaxy cluster mergers** dissipate a gravitational binding energy of

$$E_{\text{pot}} \simeq \frac{3}{5} \frac{GM_{\text{cl}}^2}{r_{\text{cl}}} \simeq 2.6 \times 10^{64} \text{ erg} \left(\frac{M_{\text{cl}}}{10^{15} M_{\odot}} \right)^2 \left(\frac{r_{\text{cl}}}{2 \text{ Mpc}} \right)^{-1}$$

- **Galaxy mergers** dissipate a gravitational binding energy of

$$E_{\text{pot}} \simeq \frac{3}{5} \frac{GM_{\text{gal}}^2}{r_{\text{gal}}} \simeq 2.1 \times 10^{59} \text{ erg} \left(\frac{M_{\text{gal}}}{10^{12} M_{\odot}} \right)^2 \left(\frac{r_{\text{gal}}}{250 \text{ kpc}} \right)^{-1}$$



Energetics of cluster mergers

- **Galaxy cluster mergers** dissipate a gravitational binding energy of

$$E_{\text{pot}} \simeq \frac{3}{5} \frac{GM_{\text{cl}}^2}{r_{\text{cl}}} \simeq 2.6 \times 10^{64} \text{ erg} \left(\frac{M_{\text{cl}}}{10^{15} M_{\odot}} \right)^2 \left(\frac{r_{\text{cl}}}{2 \text{ Mpc}} \right)^{-1}$$

- **Galaxy mergers** dissipate a gravitational binding energy of

$$E_{\text{pot}} \simeq \frac{3}{5} \frac{GM_{\text{gal}}^2}{r_{\text{gal}}} \simeq 2.1 \times 10^{59} \text{ erg} \left(\frac{M_{\text{gal}}}{10^{12} M_{\odot}} \right)^2 \left(\frac{r_{\text{gal}}}{250 \text{ kpc}} \right)^{-1}$$

- **Supernova explosions** release a gravitational binding energy as the neutron star is forming of

$$E_{\text{pot}} \simeq \frac{3}{5} \frac{GM_{\star}^2}{r_{\star}} \simeq 2.4 \times 10^{53} \text{ erg} \left(\frac{M_{\star}}{1.5 M_{\odot}} \right)^2 \left(\frac{r_{\star}}{15 \text{ km}} \right)^{-1}$$

of which most is radiated in neutrinos and only $\sim 10^{51}$ erg is available as kinetic energy to drive the shock into the ISM



Energetics of cluster mergers

- **Galaxy cluster mergers** dissipate a gravitational binding energy of

$$E_{\text{pot}} \simeq \frac{3}{5} \frac{GM_{\text{cl}}^2}{r_{\text{cl}}} \simeq 2.6 \times 10^{64} \text{ erg} \left(\frac{M_{\text{cl}}}{10^{15} M_{\odot}} \right)^2 \left(\frac{r_{\text{cl}}}{2 \text{ Mpc}} \right)^{-1}$$

- **Galaxy mergers** dissipate a gravitational binding energy of

$$E_{\text{pot}} \simeq \frac{3}{5} \frac{GM_{\text{gal}}^2}{r_{\text{gal}}} \simeq 2.1 \times 10^{59} \text{ erg} \left(\frac{M_{\text{gal}}}{10^{12} M_{\odot}} \right)^2 \left(\frac{r_{\text{gal}}}{250 \text{ kpc}} \right)^{-1}$$

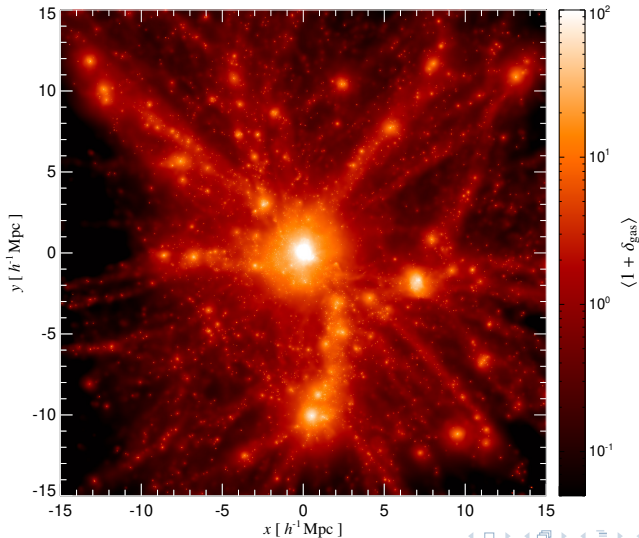
- **Supernova explosions** release a gravitational binding energy as the neutron star is forming of

$$E_{\text{pot}} \simeq \frac{3}{5} \frac{GM_{\star}^2}{r_{\star}} \simeq 2.4 \times 10^{53} \text{ erg} \left(\frac{M_{\star}}{1.5 M_{\odot}} \right)^2 \left(\frac{r_{\star}}{15 \text{ km}} \right)^{-1}$$

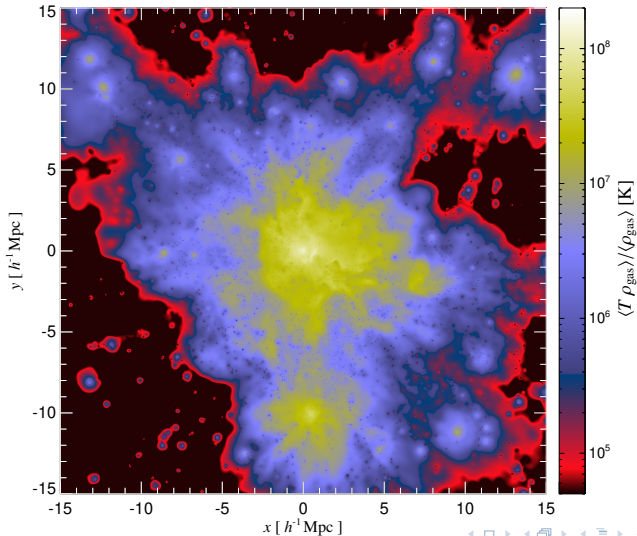
of which most is radiated in neutrinos and only $\sim 10^{51}$ erg is available as kinetic energy to drive the shock into the ISM

⇒ **cluster mergers are the most energetic events** (after the Big Bang)

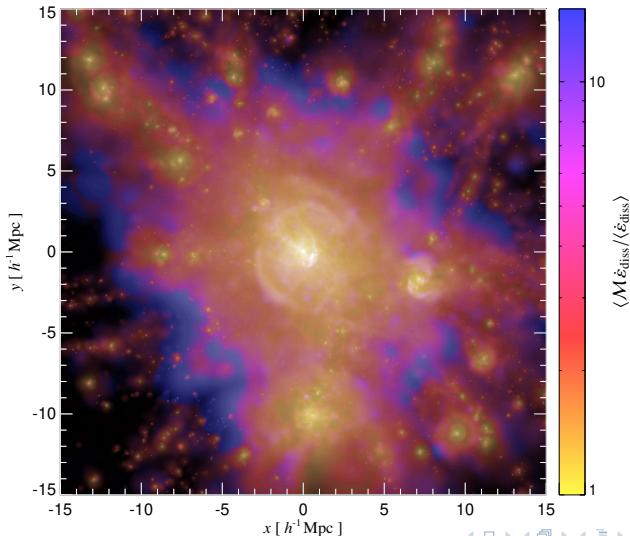
Cosmological cluster simulation: gas density



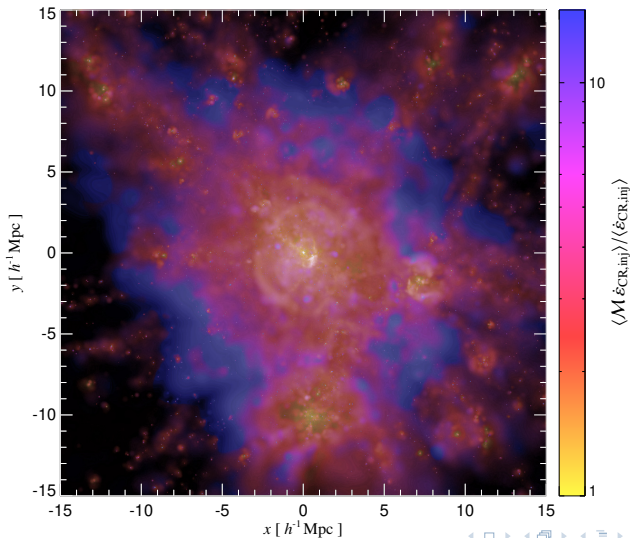
Mass weighted temperature



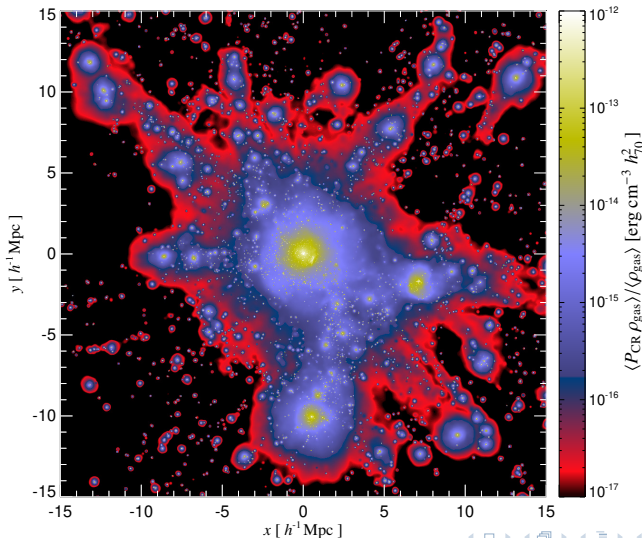
Shock strengths weighted by dissipated energy



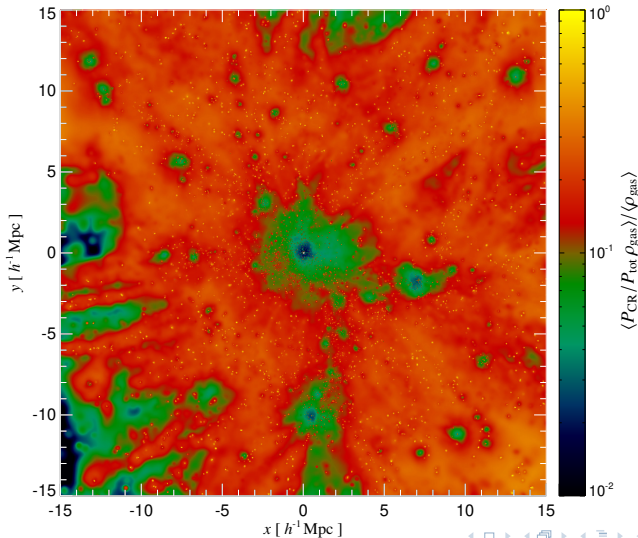
Shock strengths weighted by injected CR energy



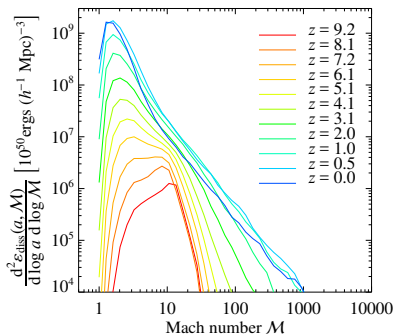
Evolved CR pressure



Relative CR pressure $P_{\text{CR}}/P_{\text{total}}$

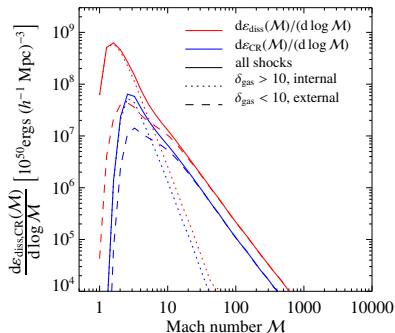
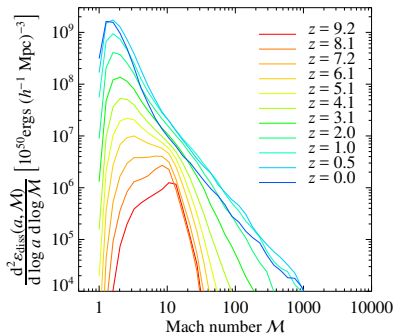


Cosmological shock statistics



- more energy is dissipated at later times
- mean Mach number decreases with time

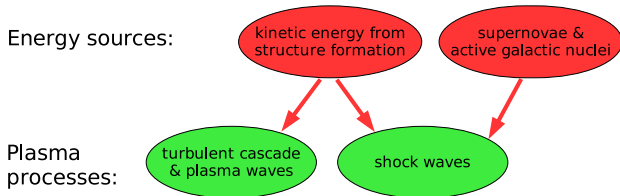
Cosmological shock statistics: CR acceleration



- more energy is dissipated in weak shocks internal to collapsed structures than in external strong shocks
- injected CR energy within clusters only makes up a small fraction of the total dissipated energy

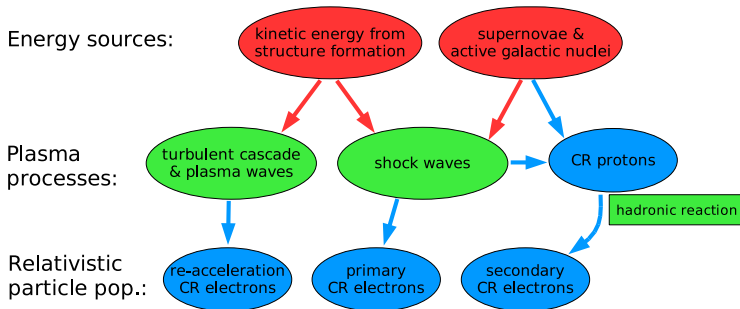
Multi messenger approach for non-thermal processes

Relativistic populations and radiative processes in clusters:

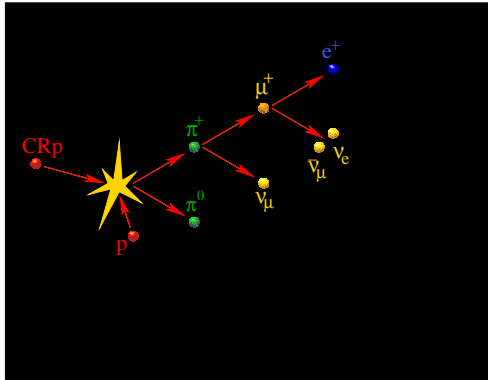


Multi messenger approach for non-thermal processes

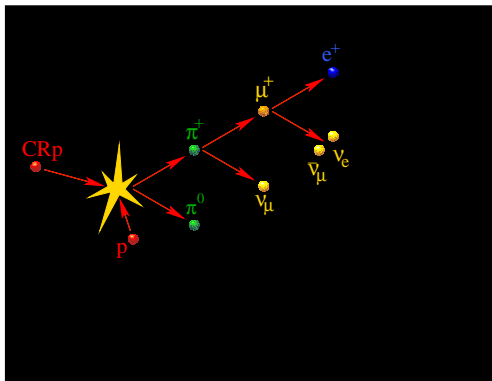
Relativistic populations and radiative processes in clusters:



Hadronic cosmic ray proton interaction



Hadronic cosmic ray proton interaction

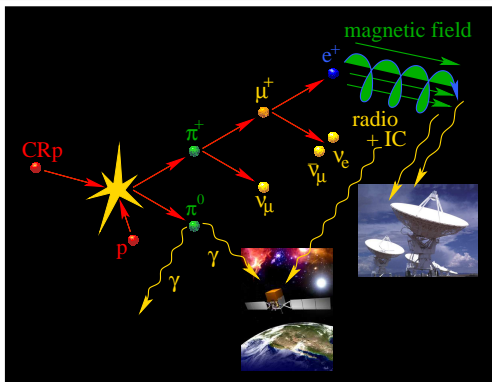


- **decay kinematics** \Rightarrow mean energy of gamma ray and secondary electrons:

$$\langle E_\gamma \rangle = \frac{1}{2} \langle E_{\pi^0} \rangle \simeq \frac{1}{8} E_p \quad \text{and} \quad \langle E_{e^\pm} \rangle = \frac{1}{4} \langle E_{\pi^\pm} \rangle \simeq \frac{1}{16} E_p,$$

where inverse multiplicity $\frac{1}{2} \times$ inelasticity $\frac{1}{2} = \frac{1}{4}$

Hadronic cosmic ray proton interaction



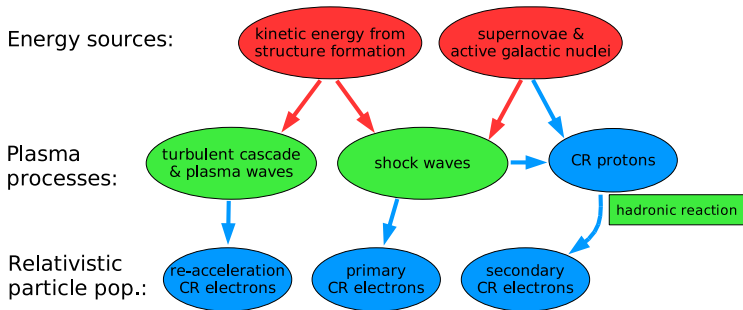
- **decay kinematics** \Rightarrow mean energy of gamma ray and secondary electrons:

$$\langle E_\gamma \rangle = \frac{1}{2} \langle E_{\pi^0} \rangle \simeq \frac{1}{8} E_p \quad \text{and} \quad \langle E_{e^\pm} \rangle = \frac{1}{4} \langle E_{\pi^\pm} \rangle \simeq \frac{1}{16} E_p,$$

where inverse multiplicity $\frac{1}{2} \times$ inelasticity $\frac{1}{2} = \frac{1}{4}$

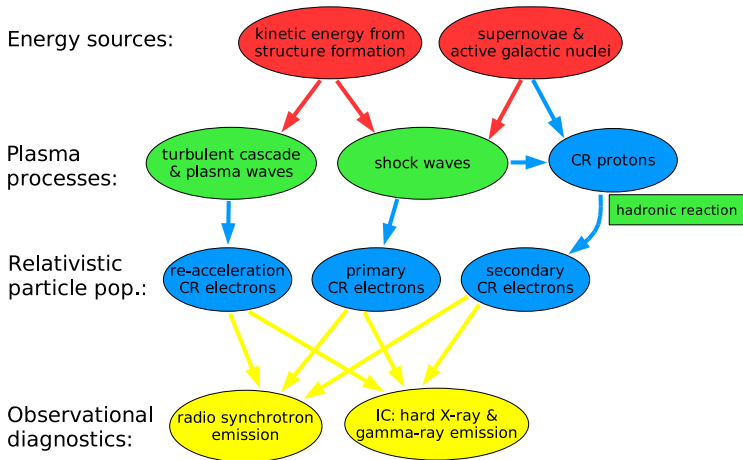
Multi messenger approach for non-thermal processes

Relativistic populations and radiative processes in clusters:



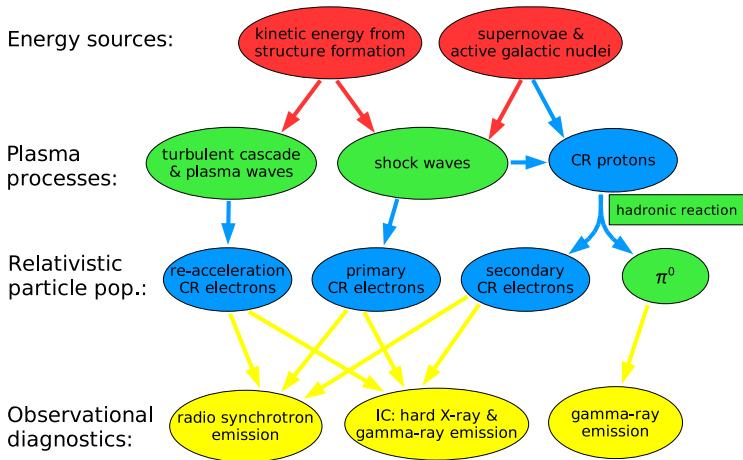
Multi messenger approach for non-thermal processes

Relativistic populations and radiative processes in clusters:



Multi messenger approach for non-thermal processes

Relativistic populations and radiative processes in clusters:



Hadronic and Coulomb cooling of ions

- **hadronic cooling time:**

$$t_{pp} = \frac{1}{0.5\sigma_{pp} n_n c}$$

where $\sigma_{pp} = 32$ mbarn is the inelastic proton cross section with an inelasticity 0.5 and $n_n = \rho/m_p$ is the number density of target nucleons

Hadronic and Coulomb cooling of ions

- **hadronic cooling time:**

$$t_{pp} = \frac{1}{0.5\sigma_{pp} n_n c}$$

where $\sigma_{pp} = 32$ mbarn is the inelastic proton cross section with an inelasticity 0.5 and $n_n = \rho/m_p$ is the number density of target nucleons

- **Coulomb cooling timescale:**

$$t_{\text{Coul},i} = \frac{E}{|\dot{E}|_{\text{Coul},i}} \approx t_d^{\text{ei}} \frac{m_i}{m_e} = \frac{m_i}{m_e n_e v_i \sigma_{ei}} = \frac{m_i}{m_e n_e v_i 2\pi b_0^2 \ln \Lambda} = \frac{m_i v_i^3}{8\pi m_e n_e r_0^2 c^4 \ln \Lambda},$$

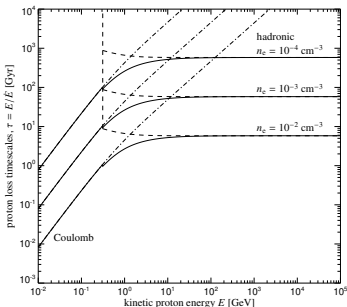
where t_d^{ei} and v_i are the deflection time and relative velocity of a CR ion and thermal electron, n_e is the electron number density, $r_0 = Ze^2/(m_e c^2)$ is the classical electron radius, $\ln \Lambda \sim 35-40$ is the Coulomb logarithm, and

$$b_0 = \frac{2Ze^2}{m_e v_i^2} = \frac{2r_0 c^2}{v_i^2}$$

is the critical impact parameter for a (rare) large-angle scattering event



Cooling times of protons

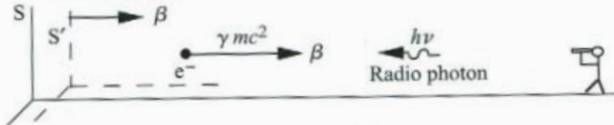
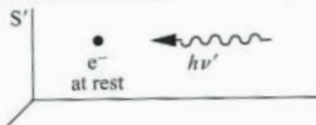
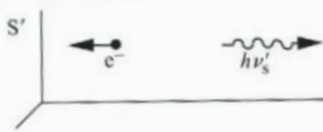


EnBlin+ (2011)

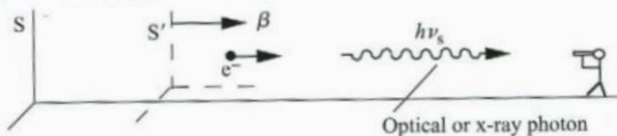
- **CR protons** thermalize their low-energy particles via Coulomb/ionization interactions, but retain their (pressure carrying) population above GeV energies because of small hadronic losses

Inverse Compton interaction – 1

(a) Before collision in S

(b) Before collision in S' (c) After collision in S' 

(d) After collision in S



Inverse Compton interaction – 2

- energy exchange between CR electron of energy $E_e = \gamma_e m_e c^2$ and a low-energy photon of energy E :

- * Lorentz boosting into the electron rest frame: $E' = \gamma_e E (1 - \beta_e \cos \theta)$

- * elastic scattering in the electron rest frame: $E'_1 = E'$

- * Lorentz de-boosting into the lab frame: $E_1 = \gamma_e E'_1 (1 + \beta_e \cos \theta'_1)$



Inverse Compton interaction – 2

- energy exchange between CR electron of energy $E_e = \gamma_e m_e c^2$ and a low-energy photon of energy E :

- * Lorentz boosting into the electron rest frame: $E' = \gamma_e E (1 - \beta_e \cos \theta)$

- * elastic scattering in the electron rest frame: $E'_1 = E'$

- * Lorentz de-boosting into the lab frame: $E_1 = \gamma_e E'_1 (1 + \beta_e \cos \theta'_1)$

- the net photon energy gain = CR electron loss is (for all but very small angles):

$$E_1 \sim \gamma_e^2 E \quad \Rightarrow \quad \langle E_1 \rangle = \frac{4}{3} \gamma_e^2 \langle E \rangle$$

Inverse Compton interaction – 2

- energy exchange between CR electron of energy $E_e = \gamma_e m_e c^2$ and a low-energy photon of energy E :

- * Lorentz boosting into the electron rest frame: $E' = \gamma_e E (1 - \beta_e \cos \theta)$

- * elastic scattering in the electron rest frame: $E'_1 = E'$

- * Lorentz de-boosting into the lab frame: $E_1 = \gamma_e E'_1 (1 + \beta_e \cos \theta'_1)$

- the net photon energy gain = CR electron loss is (for all but very small angles):

$$E_1 \sim \gamma_e^2 E \Rightarrow \langle E_1 \rangle = \frac{4}{3} \gamma_e^2 \langle E \rangle$$

- the inverse Compton energy loss rate of a CR electron

$$\dot{E}_e = -\sigma_T c n_{\text{ph}} \langle E_1 \rangle = -\frac{4}{3} \sigma_T c \varepsilon_{\text{ph}} \gamma_e^2 = -\frac{\sigma_T c}{6\pi} B_{\text{ph}}^2 \gamma_e^2,$$

where $\varepsilon_{\text{ph}} = \langle E \rangle n_{\text{ph}} = B_{\text{ph}}^2 / (8\pi)$ and σ_T is the Thomson cross section



Inverse Compton and synchrotron cooling

The energy loss rate of a relativistic electron of energy $E_e = \gamma_e m_e c^2$ is given by

$$\dot{E}_e = -\frac{\sigma_T c}{6\pi} (B_{\text{cmb}}^2 + B^2) \gamma_e^2 \quad \Rightarrow \quad t_{\text{cool}} = \frac{E_e}{|\dot{E}_e|} = \frac{6\pi m_e c}{\sigma_T (B_{\text{cmb}}^2 + B^2) \gamma_e}$$

where B is the magnetic field strength and $B_{\text{cmb}} \simeq 3.2 \mu\text{G}$ is the equivalent field of the cosmic microwave background (cmb) energy density today:

Inverse Compton and synchrotron cooling

The energy loss rate of a relativistic electron of energy $E_e = \gamma_e m_e c^2$ is given by

$$\dot{E}_e = -\frac{\sigma_T c}{6\pi} (B_{\text{cmb}}^2 + B^2) \gamma_e^2 \quad \Rightarrow \quad t_{\text{cool}} = \frac{E_e}{|\dot{E}_e|} = \frac{6\pi m_e c}{\sigma_T (B_{\text{cmb}}^2 + B^2) \gamma_e}$$

where B is the magnetic field strength and $B_{\text{cmb}} \simeq 3.2 \mu\text{G}$ is the equivalent field of the cosmic microwave background (cmb) energy density today:

- the first term $\propto B_{\text{cmb}}^2$ describes energy loss due to inverse Compton (IC) scattering off of CMB photons, while the second term $\propto B^2$ describes energy loss due to synchrotron emission

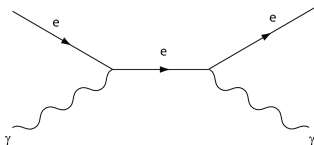
Inverse Compton and synchrotron cooling

The energy loss rate of a relativistic electron of energy $E_e = \gamma_e m_e c^2$ is given by

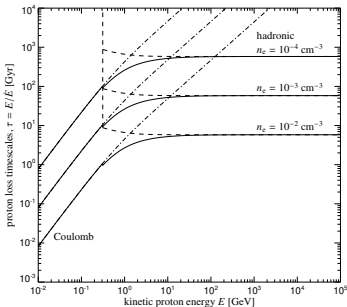
$$\dot{E}_e = -\frac{\sigma_T c}{6\pi} (B_{\text{cmb}}^2 + B^2) \gamma_e^2 \Rightarrow t_{\text{cool}} = \frac{E_e}{|\dot{E}_e|} = \frac{6\pi m_e c}{\sigma_T (B_{\text{cmb}}^2 + B^2) \gamma_e}$$

where B is the magnetic field strength and $B_{\text{cmb}} \simeq 3.2 \mu\text{G}$ is the equivalent field of the cosmic microwave background (cmb) energy density today:

- the first term $\propto B_{\text{cmb}}^2$ describes energy loss due to inverse Compton (IC) scattering off of CMB photons, while the second term $\propto B^2$ describes energy loss due to synchrotron emission
- the structural similarity of the formulae is not a coincidence but caused by the same Feynman diagram of the scattering process: while IC emission evokes real photons, synchrotron emission borrows a virtual photon from the magnetic field



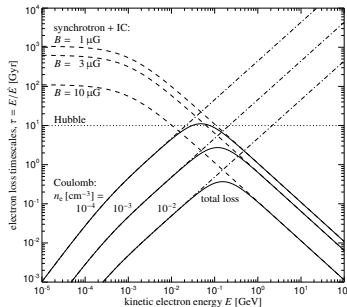
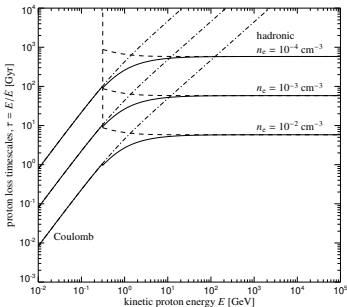
Cooling times of protons



EnBlin+ (2011)

- **CR protons** thermalize their low-energy particles via Coulomb/ionization interactions, but retain their (pressure carrying) population above GeV energies because of small hadronic losses

Cooling times of protons and electrons

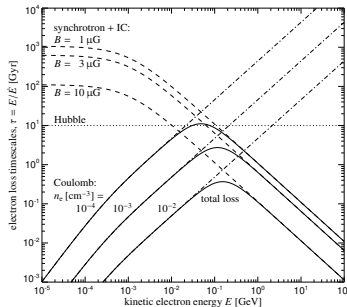
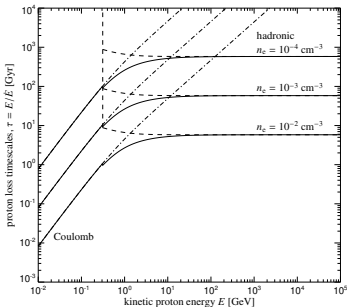


EnBlin+ (2011)

- **CR protons** thermalize their low-energy particles via Coulomb/ionization interactions, but retain their (pressure carrying) population above GeV energies because of small hadronic losses
- **CR electrons** at Lorenz factors $\gamma_e \lesssim 100$ are thermalized via Coulomb interactions and high-energy electrons quickly lose energy via synchrotron/inverse Compton interactions



Cooling times of protons and electrons



EnBlin+ (2011)

- **CR protons** thermalize their low-energy particles via Coulomb/ionization interactions, but retain their (pressure carrying) population above GeV energies because of small hadronic losses
- **CR electrons** at Lorenz factors $\gamma_e \lesssim 100$ are thermalized via Coulomb interactions and high-energy electrons quickly lose energy via synchrotron/inverse Compton interactions
 \Rightarrow **bottleneck at $\gamma_e \sim 100$ causes accumulation of fossil CR electrons**



Electron cooling and synchrotron emission

- the cooling time $t_{\text{cool}} = E_e / |\dot{E}_e|$ of a relativistic electron is given by

$$t_{\text{cool}} = \frac{E_e}{|\dot{E}_e|} = \frac{6\pi m_e c}{\sigma_T (B_{\text{cmb}}^2 + B^2) \gamma_e} \approx 200 \text{ Myr},$$

for $B = 1 \mu\text{G}$ and $\gamma_e = 10^4$

Electron cooling and synchrotron emission

- the cooling time $t_{\text{cool}} = E_e / |\dot{E}_e|$ of a relativistic electron is given by

$$t_{\text{cool}} = \frac{E_e}{|\dot{E}_e|} = \frac{6\pi m_e c}{\sigma_T (B_{\text{cmb}}^2 + B^2) \gamma_e} \approx 200 \text{ Myr},$$

for $B = 1 \mu\text{G}$ and $\gamma_e = 10^4$

- the synchrotron frequency in the monochromatic approximation is given by

$$\nu_{\text{syn}} = \frac{3eB}{2\pi m_e c} \gamma_e^2 \simeq 1 \text{ GHz} \frac{B}{\mu\text{G}} \left(\frac{\gamma_e}{10^4} \right)^2$$

Electron cooling and synchrotron emission

- the cooling time $t_{\text{cool}} = E_e / |\dot{E}_e|$ of a relativistic electron is given by

$$t_{\text{cool}} = \frac{E_e}{|\dot{E}_e|} = \frac{6\pi m_e c}{\sigma_T (B_{\text{cmb}}^2 + B^2) \gamma_e} \approx 200 \text{ Myr},$$

for $B = 1 \mu\text{G}$ and $\gamma_e = 10^4$

- the synchrotron frequency in the monochromatic approximation is given by

$$\nu_{\text{syn}} = \frac{3eB}{2\pi m_e c} \gamma_e^2 \simeq 1 \text{ GHz} \frac{B}{\mu\text{G}} \left(\frac{\gamma_e}{10^4} \right)^2$$

- combining both equations by eliminating the Lorentz factor γ_e yields the cooling time of electrons that emit at frequency ν_{syn} ,

$$t_{\text{cool}} = \frac{\sqrt{54\pi m_e c e B \nu_{\text{syn}}^{-1}}}{\sigma_T (B_{\text{cmb}}^2 + B^2)} \lesssim 190 \left(\frac{\nu_{\text{syn}}}{1.4 \text{ GHz}} \right)^{-1/2} \text{ Myr}$$

\Rightarrow the cooling time t_{cool} is then bound from above and attains its maximum cooling time at $B = B_{\text{cmb},0} / \sqrt{3} \simeq 1.8 \mu\text{G}$, independent of the magnetic field



Equilibrium distribution of CR electrons

- **CR electron acceleration:** in galaxies, CR electrons are either directly accelerated at supernova remnant shocks or in hadronic CR proton interactions
→ source function $s_e = CE_e^{-\alpha_e}$, with $\alpha_e \simeq 2 - 2.4$

Equilibrium distribution of CR electrons

- **CR electron acceleration:** in galaxies, CR electrons are either directly accelerated at supernova remnant shocks or in hadronic CR proton interactions
→ source function $s_e = CE_e^{-\alpha_e}$, with $\alpha_e \simeq 2 - 2.4$
- **CR electron cooling:** at high energies, synchrotron and inverse Compton (IC) interactions with starlight & CMB photons dominate the losses:

$$\dot{E}_e(E_e) = -\frac{4}{3} \frac{\sigma_T c}{m_e^2 c^4} [\varepsilon_B + \varepsilon_{\text{ph}}] E_e^2$$



Equilibrium distribution of CR electrons

- **CR electron acceleration:** in galaxies, CR electrons are either directly accelerated at supernova remnant shocks or in hadronic CR proton interactions → source function $s_e = CE_e^{-\alpha_e}$, with $\alpha_e \simeq 2 - 2.4$
- **CR electron cooling:** at high energies, synchrotron and inverse Compton (IC) interactions with starlight & CMB photons dominate the losses:

$$\dot{E}_e(E_e) = -\frac{4}{3} \frac{\sigma_T c}{m_e^2 c^4} [\varepsilon_B + \varepsilon_{ph}] E_e^2$$

- **in steady state, CR electron acceleration balances cooling** via synchrotron and IC processes:

$$\frac{\partial}{\partial E_e} \left[\dot{E}_e(E_e) f_e(E_e) \right] = s_e(E_e)$$

Equilibrium distribution of CR electrons

- **CR electron acceleration:** in galaxies, CR electrons are either directly accelerated at supernova remnant shocks or in hadronic CR proton interactions
 → source function $s_e = CE_e^{-\alpha_e}$, with $\alpha_e \simeq 2 - 2.4$
- **CR electron cooling:** at high energies, synchrotron and inverse Compton (IC) interactions with starlight & CMB photons dominate the losses:

$$\dot{E}_e(E_e) = -\frac{4}{3} \frac{\sigma_T c}{m_e^2 c^4} [\varepsilon_B + \varepsilon_{ph}] E_e^2$$

- **in steady state, CR electron acceleration balances cooling** via synchrotron and IC processes:

$$\frac{\partial}{\partial E_e} [\dot{E}_e(E_e) f_e(E_e)] = s_e(E_e)$$

- **solution:** for $\dot{E}_e(E_e) < 0$, this equation is solved by

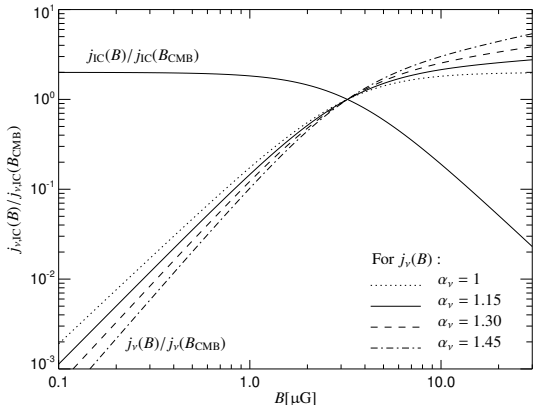
$$f_e(E_e) = \frac{1}{|\dot{E}_e(E_e)|} \int_{E_e}^{\infty} dE'_e s_e(E'_e) = \frac{C}{(\alpha_e - 1) |\dot{E}_e(E_e)|} E_e^{1-\alpha_e} \propto E_e^{-\alpha_e-1}$$

where we assumed synchrotron/IC loss processes in the last step



Synchrotron vs. inverse Compton emissivity

In steady state, the emissivity in the IC/synchrotron regime is nearly independent of B



inverse Compton cooling regime: $B < B_{\text{CMB}} \simeq 3.2(1+z)^2 \mu\text{G}$,

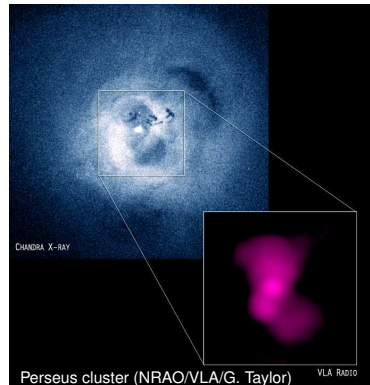
synchrotron cooling regime: $B > B_{\text{CMB}}$.

Overview of diffuse radio phenomenon

- **radio relics:** located at cluster periphery, irregular morphology, $\alpha_\nu \sim 1-2.5$, where $j_\nu \propto \nu^{-\alpha_\nu}$, polarized
 - **radio relic bubble:** aged radio cocoon, steep spectrum
 - **radio phoenix:** shock-revived bubble that has already faded out of the radio window \rightarrow *adiabatic compression?*
 - **radio gischt:** irregular morphology, at cluster periphery ($< \text{Mpc}$), in some cases coincident with weak X-ray shock, polarized \rightarrow *diffusive shock acceleration (Fermi I)*

AGN bubbles and relic relativistic plasma

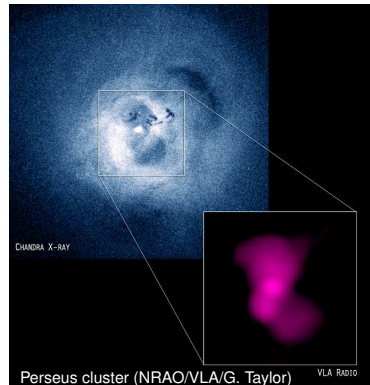
Paradigm: super-massive black holes with $M_{\bullet} \sim (10^9 - 10^{10}) M_{\odot}$ co-evolve with their hosting cD galaxies at the centers of galaxy clusters. They launch relativistic jets that potentially provide energetic feedback to balance cooling as in the active galactic nucleus (AGN) in NGC 1275, the cD galaxy in the Perseus cluster.



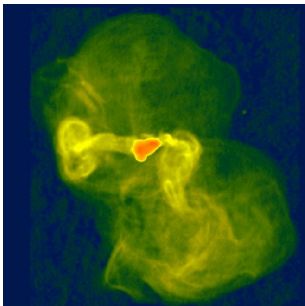
AGN bubbles and relic relativistic plasma

Paradigm: super-massive black holes with $M_{\bullet} \sim (10^9 - 10^{10}) M_{\odot}$ co-evolve with their hosting cD galaxies at the centers of galaxy clusters. They launch relativistic jets that potentially provide energetic feedback to balance cooling as in the active galactic nucleus (AGN) in NGC 1275, the cD galaxy in the Perseus cluster.

- **AGN jets inflate radio lobes** upon interacting with the ambient ICM
- **jet/lobes provide $p d V$ work** that push the X-ray emitting gas away
- **light bubbles are filled with non-thermal components and rise buoyantly**, relativistic electrons cool via synchrotron emission
- **when relativistic electrons have cooled sufficiently, lobes become invisible in the radio band:** X-ray cavities with “ghost bubbles” south and north-west to NGC 1275



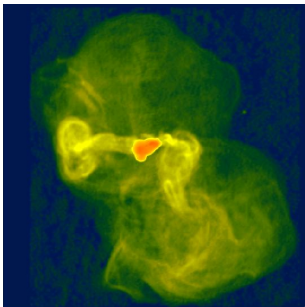
Messier 87 at radio wavelengths



$\nu = 1.4$ GHz (Owen+ 2000)

- high- ν : freshly accelerated CR electrons
- low- ν : fossil CR electrons \rightarrow time-integrated AGN feedback!

Messier 87 at radio wavelengths



$\nu = 1.4$ GHz (Owen+ 2000)



$\nu = 140$ MHz (LOFAR/de Gasperin+ 2012)

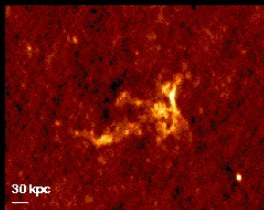
- high- ν : freshly accelerated CR electrons
- low- ν : fossil CR electrons \rightarrow time-integrated AGN feedback!
- LOFAR: halo confined to same region at all frequencies and no low- ν spectral steepening \rightarrow puzzle of “missing fossil electrons”
- solution: electrons are fully mixed with the dense cluster gas and cooled through Coulomb interactions

Radio phoenix

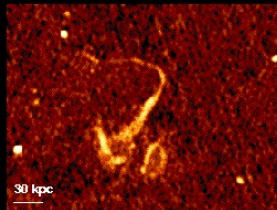
Cluster Relic Radio Sources

VLA 1.4 GHz

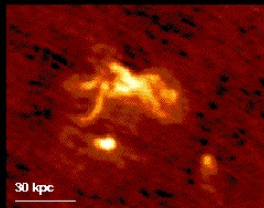
Abell 13



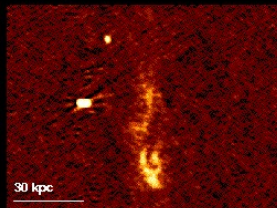
Abell 85



Abell 133

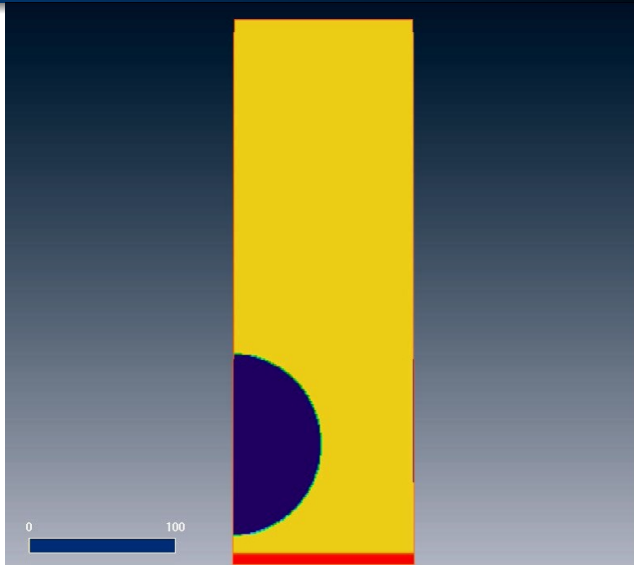


Abell 4038

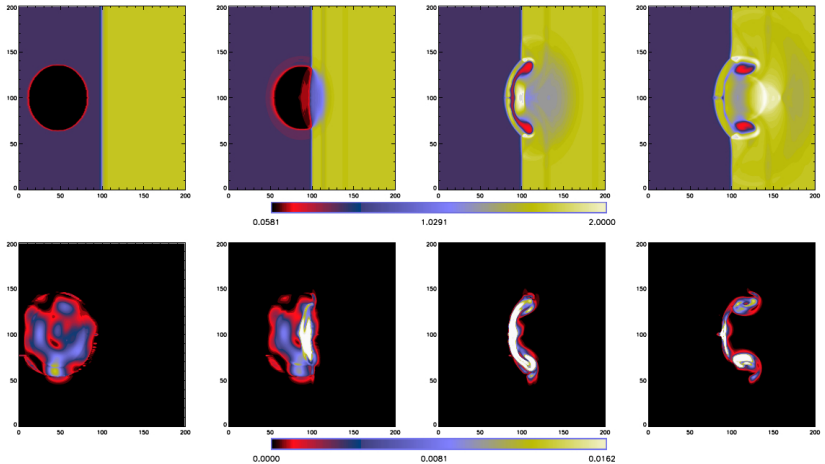


Slee, Roy, Murgia, Andernach & Ehle 2001

Shock overruns an aged radio bubble (Pfrommer & Jones 2011)



Bubble transformation to vortex ring



Enßlin & Brüggen (2002): gas density (*top*) and magnetic energy density (*bottom*)

Radio phoenix rising from the ashes of ghost bubbles

- **shock transforms bubble into torus** and adiabatically compresses the CR electrons and the magnetic field strength \Rightarrow revives invisible radio emission

Radio phoenix rising from the ashes of ghost bubbles

- **shock transforms bubble into torus** and adiabatically compresses the CR electrons and the magnetic field strength \Rightarrow revives invisible radio emission
- **the compression factor equals the volume change** (assuming that the bubble radius is invariant for this transition):

$$C = \frac{V_{\text{bubble}}}{V_{\text{torus}}} = \frac{\frac{4}{3}\pi R^3}{2\pi^2 R r_{\text{min}}^2} = \frac{2}{3\pi} \left(\frac{R}{r_{\text{min}}} \right)^2,$$

where r_{min} is the minor radius of the torus



Radio phoenix rising from the ashes of ghost bubbles

- **shock transforms bubble into torus** and adiabatically compresses the CR electrons and the magnetic field strength \Rightarrow revives invisible radio emission
- **the compression factor equals the volume change** (assuming that the bubble radius is invariant for this transition):

$$C = \frac{V_{\text{bubble}}}{V_{\text{torus}}} = \frac{\frac{4}{3}\pi R^3}{2\pi^2 R r_{\text{min}}^2} = \frac{2}{3\pi} \left(\frac{R}{r_{\text{min}}} \right)^2,$$

where r_{min} is the minor radius of the torus

- **the pressures of CR electrons and magnetic field are adiabatically compressed** across the shock passage:

$$P_{\text{CRe}} = P_{\text{CRe},0} C^{4/3} \quad \text{and} \quad P_B = P_{B,0} C^{4/3}$$



Radio phoenix rising from the ashes of ghost bubbles

- **shock transforms bubble into torus** and adiabatically compresses the CR electrons and the magnetic field strength \Rightarrow revives invisible radio emission
- **the compression factor equals the volume change** (assuming that the bubble radius is invariant for this transition):

$$C = \frac{V_{\text{bubble}}}{V_{\text{torus}}} = \frac{\frac{4}{3}\pi R^3}{2\pi^2 R r_{\text{min}}^2} = \frac{2}{3\pi} \left(\frac{R}{r_{\text{min}}} \right)^2,$$

where r_{min} is the minor radius of the torus

- **the pressures of CR electrons and magnetic field are adiabatically compressed** across the shock passage:

$$P_{\text{CRe}} = P_{\text{CRe},0} C^{4/3} \quad \text{and} \quad P_B = P_{B,0} C^{4/3}$$

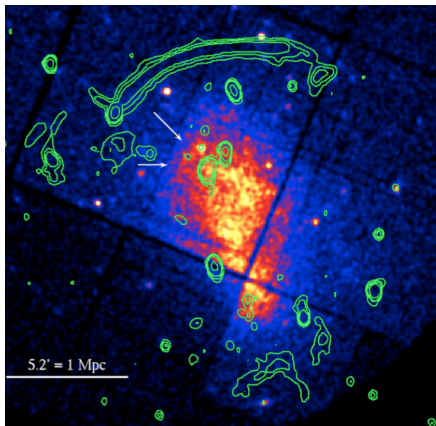
- **this boosts the radio emission**, which scales as

$$j_\nu \propto P_{\text{CRe}} P_B \propto C^{8/3} \sim 100 \dots 460$$

for a compression factor $C = 6 \dots 10$ and weak magnetic fields, $B \lesssim B_{\text{cmb}}$

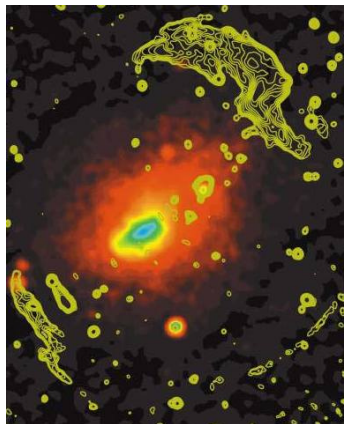


Radio gischt: double relic sources



CIZA J2242.8+5301 ("sausage relic")

X-ray: XMM, radio: WSRT/Ogrean+



Abell 3667

radio: Johnston-Hollitt, X-ray: ROSAT/PSPC

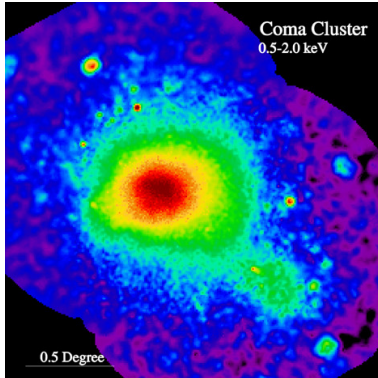
Overview of diffuse radio phenomenon

- **radio relics:** located at cluster periphery, irregular morphology, $\alpha_\nu \sim 1-2.5$, where $j_\nu \propto \nu^{-\alpha_\nu}$, polarized
 - **radio relic bubble:** aged radio cocoon, steep spectrum
 - **radio phoenix:** shock-revived bubble that has already faded out of the radio window \rightarrow *adiabatic compression?*
 - **radio gischt:** irregular morphology, at cluster periphery ($< \text{Mpc}$), in some cases coincident with weak X-ray shock, polarized \rightarrow *diffusive shock acceleration (Fermi I)*

Overview of diffuse radio phenomenon

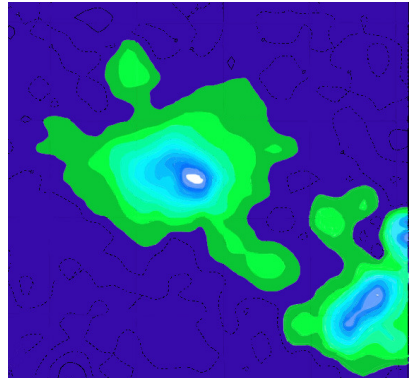
- **radio relics:** located at cluster periphery, irregular morphology, $\alpha_\nu \sim 1-2.5$, where $j_\nu \propto \nu^{-\alpha_\nu}$, polarized
 - **radio relic bubble:** aged radio cocoon, steep spectrum
 - **radio phoenix:** shock-revived bubble that has already faded out of the radio window \rightarrow *adiabatic compression?*
 - **radio gischt:** irregular morphology, at cluster periphery ($< \text{Mpc}$), in some cases coincident with weak X-ray shock, polarized \rightarrow *diffusive shock acceleration (Fermi I)*
- **radio halos:** centrally located, regular morphology (like X-rays), $\alpha_\nu \sim 1-1.5$, unpolarized
 - **giant radio halos:** occur in merging clusters, $> 1 \text{ Mpc}$ -sized, morphology similar to X-rays
 - **radio mini halos:** occur in cool core clusters, few times 100 kpc in size, emission extends over cool core

Giant radio halo in the Coma cluster



thermal X-ray emission

Snowden/MPE/ROSAT

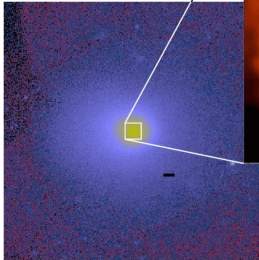


radio synchrotron emission

Deiss/Effelsberg

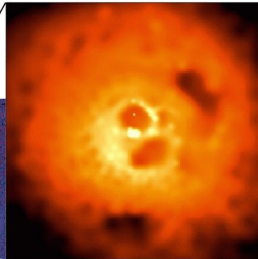
Radio mini halo in the Perseus cluster

ROSAT observation:
Perseus galaxy cluster

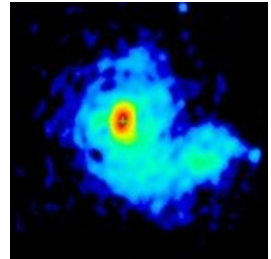


thermal X-ray emission

ROSAT, NASA/IoA/Fabian+



Chandra observation:
central region of Perseus



radio synchrotron emission

Pedlar/VLA



AIP

Overview of diffuse radio phenomenon

- **radio relics:** located at cluster periphery, irregular morphology, $\alpha_\nu \sim 1-2.5$, where $j_\nu \propto \nu^{-\alpha_\nu}$, polarized
 - **radio relic bubble:** aged radio cocoon, steep spectrum
 - **radio phoenix:** shock-revived bubble that has already faded out of the radio window \rightarrow *adiabatic compression?*
 - **radio gischt:** irregular morphology, at cluster periphery ($< \text{Mpc}$), in some cases coincident with weak X-ray shock, polarized \rightarrow *diffusive shock acceleration (Fermi I)*
- **radio halos:** centrally located, regular morphology (like X-rays), $\alpha_\nu \sim 1-1.5$, unpolarized
 - **giant radio halos:** occur in merging clusters, $> 1 \text{ Mpc}$ -sized, morphology similar to X-rays
 - **radio mini halos:** occur in cool core clusters, few times 100 kpc in size, emission extends over cool core

Giant radio relics

- recall the cooling time of electrons that emit at frequency ν_{syn} ,

$$t_{\text{cool}} = \frac{\sqrt{54\pi m_e c e B \nu_{\text{syn}}^{-1}}}{\sigma_T (B_{\text{cmb}}^2 + B^2)} \lesssim 190 \left(\frac{\nu_{\text{syn}}}{1.4 \text{ GHz}} \right)^{-1/2} \text{ Myr}$$



Giant radio relics

- recall the cooling time of electrons that emit at frequency ν_{syn} ,

$$t_{\text{cool}} = \frac{\sqrt{54\pi m_e c e B \nu_{\text{syn}}^{-1}}}{\sigma_T (B_{\text{cmb}}^2 + B^2)} \lesssim 190 \left(\frac{\nu_{\text{syn}}}{1.4 \text{ GHz}} \right)^{-1/2} \text{ Myr}$$

- assuming that (i) the relativistic electrons are accelerated at a strong cluster merger shock, (ii) are advected with the post-shock gas, and (iii) that the incoming gas had a pre-shock velocity of $v_1 = 1200 \text{ km/s}$ in the shock frame, we get a post-shock velocity

$$v_2 = \frac{\rho_1}{\rho_2} v_1 = \frac{(\gamma - 1)\mathcal{M}_1^2 + 2}{(\gamma + 1)\mathcal{M}_1^2} v_1 = 400 \left(\frac{v_1}{1200 \text{ km s}^{-1}} \right) \text{ km s}^{-1}$$

for a shock Mach number of $\mathcal{M}_1 = 3$



Giant radio relics

- recall the cooling time of electrons that emit at frequency ν_{syn} ,

$$t_{\text{cool}} = \frac{\sqrt{54\pi m_e c e B \nu_{\text{syn}}^{-1}}}{\sigma_T (B_{\text{cmb}}^2 + B^2)} \lesssim 190 \left(\frac{\nu_{\text{syn}}}{1.4 \text{ GHz}} \right)^{-1/2} \text{ Myr}$$

- assuming that (i) the relativistic electrons are accelerated at a strong cluster merger shock, (ii) are advected with the post-shock gas, and (iii) that the incoming gas had a pre-shock velocity of $v_1 = 1200 \text{ km/s}$ in the shock frame, we get a post-shock velocity

$$v_2 = \frac{\rho_1}{\rho_2} v_1 = \frac{(\gamma - 1)\mathcal{M}_1^2 + 2}{(\gamma + 1)\mathcal{M}_1^2} v_1 = 400 \left(\frac{v_1}{1200 \text{ km s}^{-1}} \right) \text{ km s}^{-1}$$

for a shock Mach number of $\mathcal{M}_1 = 3$

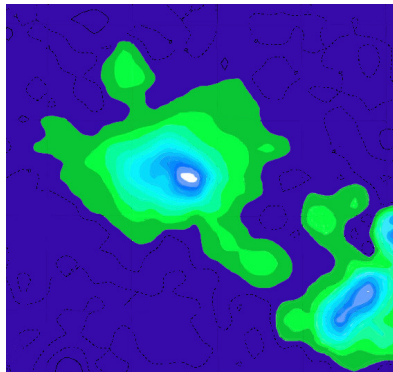
- this implies a maximum cooling length $L_{\text{cool, max}} = v_2 t_{\text{cool, max}} = 80 \text{ kpc}$, which decreases for larger magnetic field strengths to take on a value for $5 \mu\text{G}$ of

$$L_{\text{cool}} = v_2 t_{\text{cool}} = \frac{v_2 \sqrt{54\pi m_e c e B \nu_{\text{syn}}^{-1}}}{\sigma_T (B_{\text{cmb}}^2 + B^2)} \approx 30 \left(\frac{\nu_{\text{syn}}}{1.4 \text{ GHz}} \right)^{-1/2} \text{ kpc}$$

typical radial extents of radio shocks are of that size \Rightarrow use the relic geometry to estimate magnetic field strengths (projection effects!)

Giant radio halos

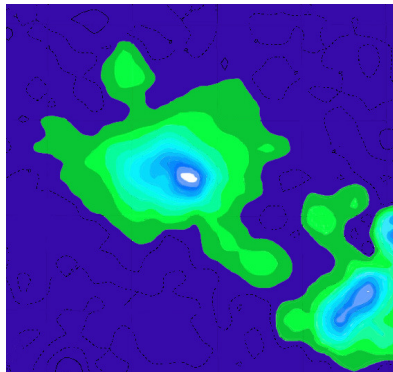
- the maximum cooling length is
 $L_{\text{cool, max}} = v_2 t_{\text{cool, max}} = 80 \text{ kpc}$ at 1.4 GHz
- the spatial extend of giant radio halos is $\sim 2 \text{ Mpc}$ and the emission is not polarized



radio synchrotron emission (Deiss/Effelsberg)

Giant radio halos

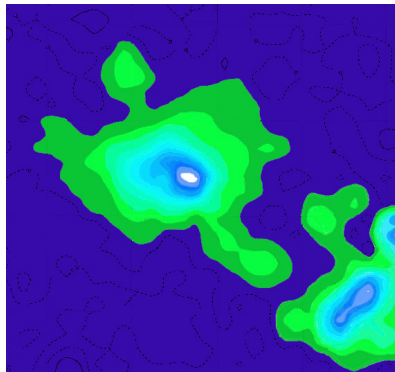
- the maximum cooling length is
 $L_{\text{cool, max}} = v_2 t_{\text{cool, max}} = 80 \text{ kpc}$ at 1.4 GHz
- the spatial extend of giant radio halos is $\sim 2 \text{ Mpc}$ and the emission is not polarized
- because synchrotron emission is intrinsically polarized, this means that the emission is a **projection of causally uncorrelated regions** along the line of sight or there is **beam depolarization**



radio synchrotron emission (Deiss/Effelsberg)

Giant radio halos

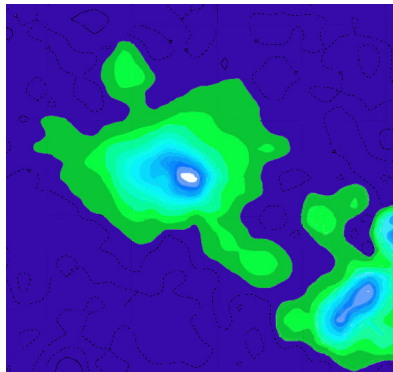
- the maximum cooling length is
 $L_{\text{cool, max}} = v_2 t_{\text{cool, max}} = 80 \text{ kpc}$ at 1.4 GHz
- the spatial extend of giant radio halos is $\sim 2 \text{ Mpc}$ and the emission is not polarized
- because synchrotron emission is intrinsically polarized, this means that the emission is a **projection of causally uncorrelated regions** along the line of sight or there is **beam depolarization**
- because $L_{\text{halo}} \approx 25 L_{\text{cool, max}}$ there must be a **volume filling acceleration process of relativistic electrons**



radio synchrotron emission (Deiss/Effelsberg)

Giant radio halos

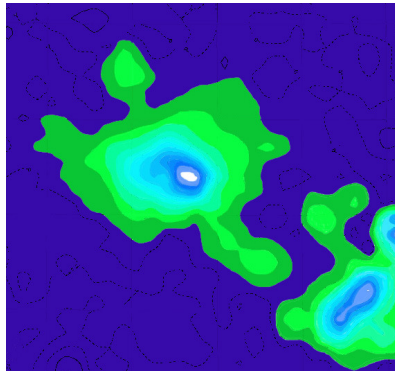
- the maximum cooling length is
 $L_{\text{cool, max}} = v_2 t_{\text{cool, max}} = 80 \text{ kpc}$ at 1.4 GHz
- the spatial extend of giant radio halos is $\sim 2 \text{ Mpc}$ and the emission is not polarized
- because synchrotron emission is intrinsically polarized, this means that the emission is a **projection of causally uncorrelated regions** along the line of sight or there is **beam depolarization**
- because $L_{\text{halo}} \approx 25 L_{\text{cool, max}}$ there must be a **volume filling acceleration process of relativistic electrons**
- hadronic model**: relativistic protons interact hadronically with gas protons and produce secondary electrons/positrons that emit in the radio



radio synchrotron emission (Deiss/Effelsberg)

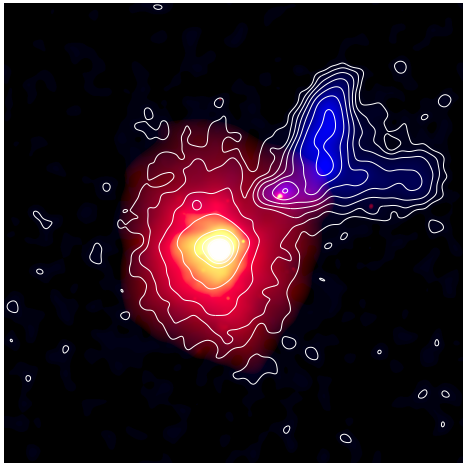
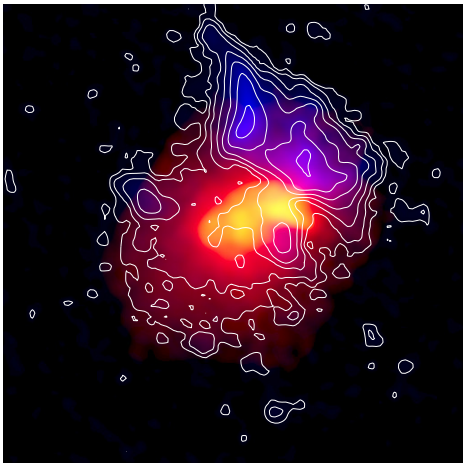
Giant radio halos

- the maximum cooling length is
 $L_{\text{cool, max}} = v_2 t_{\text{cool, max}} = 80 \text{ kpc}$ at 1.4 GHz
- the spatial extend of giant radio halos is $\sim 2 \text{ Mpc}$ and the emission is not polarized
- because synchrotron emission is intrinsically polarized, this means that the emission is a **projection of causally uncorrelated regions** along the line of sight or there is **beam depolarization**
- because $L_{\text{halo}} \approx 25 L_{\text{cool, max}}$ there must be a **volume filling acceleration process of relativistic electrons**
- hadronic model**: relativistic protons interact hadronically with gas protons and produce secondary electrons/positrons that emit in the radio
- reacceleration model**: fossil or secondary electrons interact with turbulent magneto-hydrodynamic waves and experience Fermi-II acceleration that makes them visible at radio wave lengths



radio synchrotron emission (Deiss/Effelsberg)

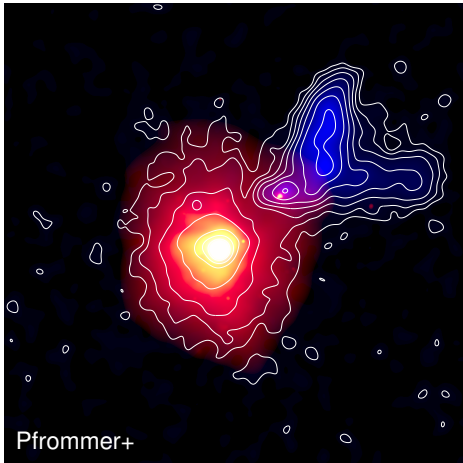
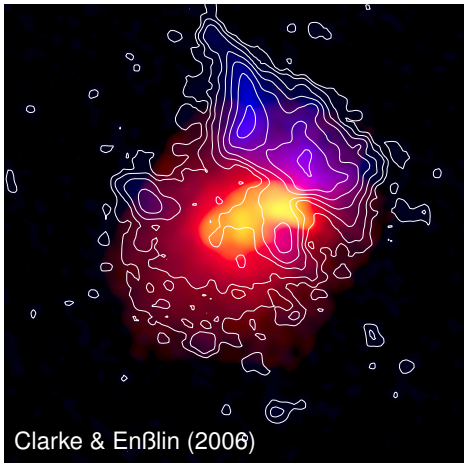
Which one is the simulation/observation of A2256?



red/yellow: thermal X-ray emission,
blue/contours: 1.4 GHz radio emission with giant radio halo and relic

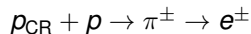


Observation – simulation of A2256



red/yellow: thermal X-ray emission,
blue/contours: 1.4 GHz radio emission with giant radio halo and relic

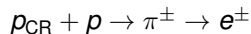
Radio halo theory – (i) hadronic model



strength:

- all required ingredients available:
shocks to inject CRp, gas protons as targets, magnetic fields
- predicted luminosities and morphologies as observed without tuning
- power-law spectra as observed

Radio halo theory – (i) hadronic model



strength:

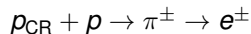
- all required ingredients available:
shocks to inject CRp, gas protons as targets, magnetic fields
- predicted luminosities and morphologies as observed without tuning
- power-law spectra as observed

weakness:

- all clusters should have radio halos
- does not explain all reported spectral features
- ...



Radio halo theory – (i) hadronic model



strength:

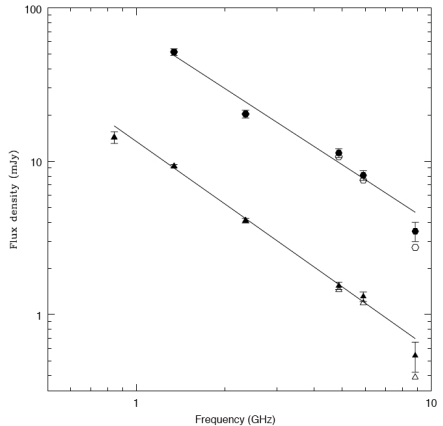
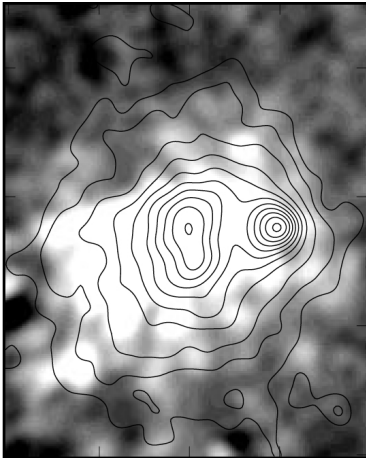
- all required ingredients available:
shocks to inject CRp, gas protons as targets, magnetic fields
- predicted luminosities and morphologies as observed without tuning
- power-law spectra as observed

weakness:

- ~~all clusters should have radio halos~~
- does not explain all reported spectral features
- ...



Radio halo and spectrum in the Bullet cluster

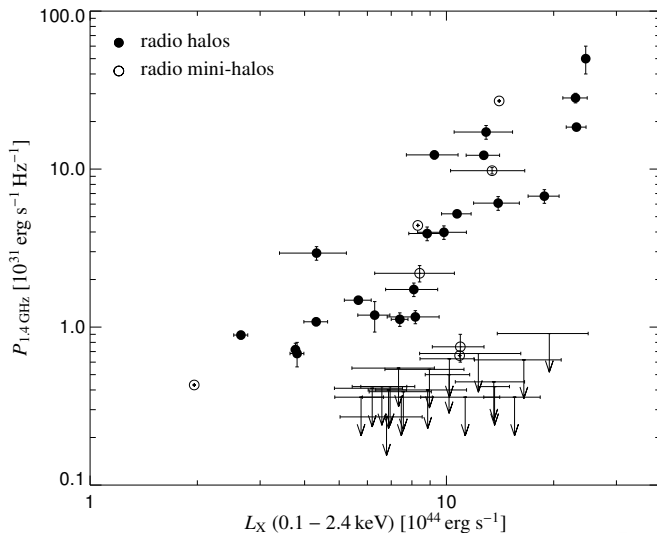


Liang et al. (2000): SZ-corrected

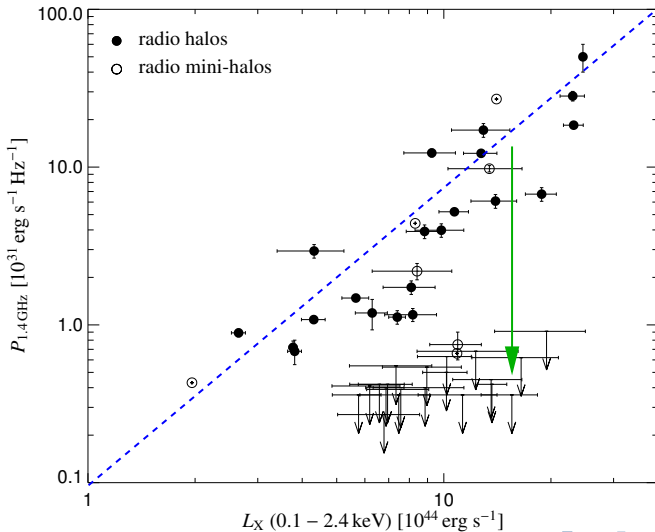


AIP

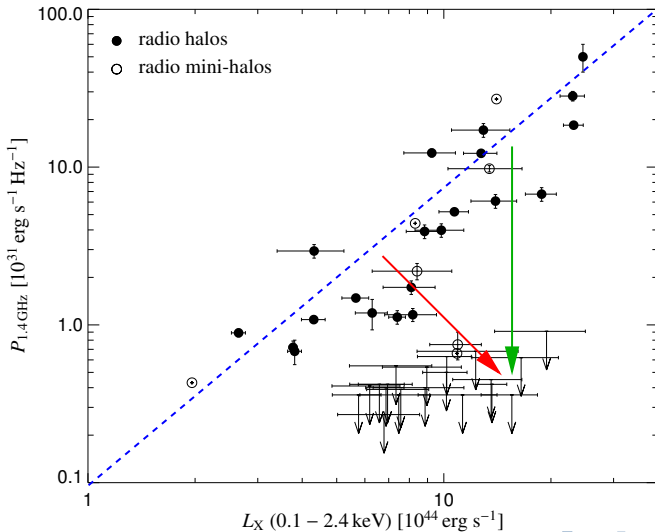
Radio luminosity - X-ray luminosity



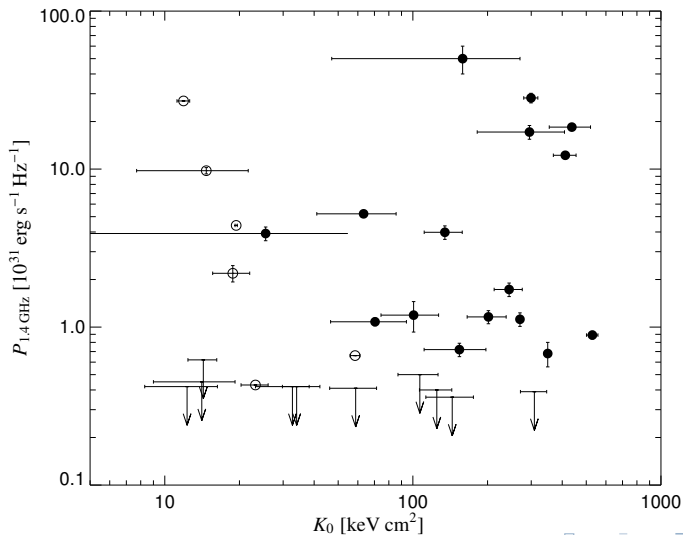
Radio luminosity - X-ray luminosity



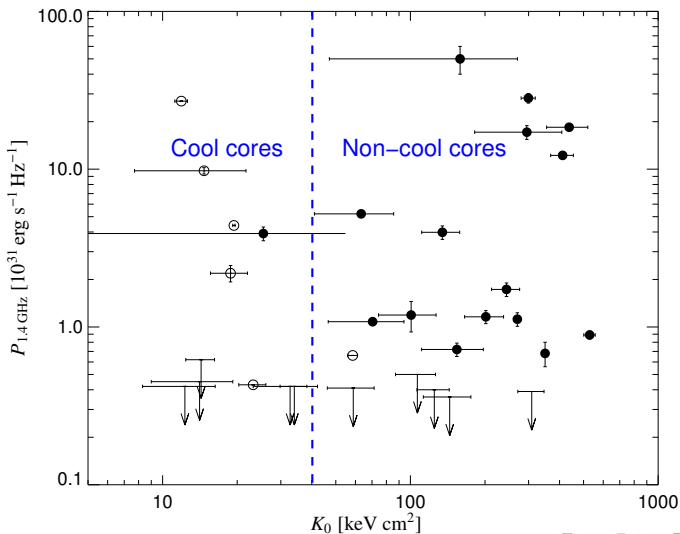
Radio luminosity - X-ray luminosity



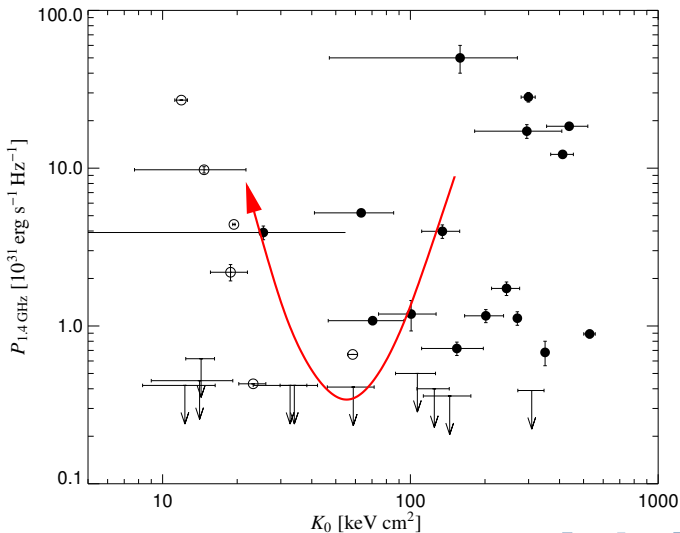
Radio luminosity - central entropy



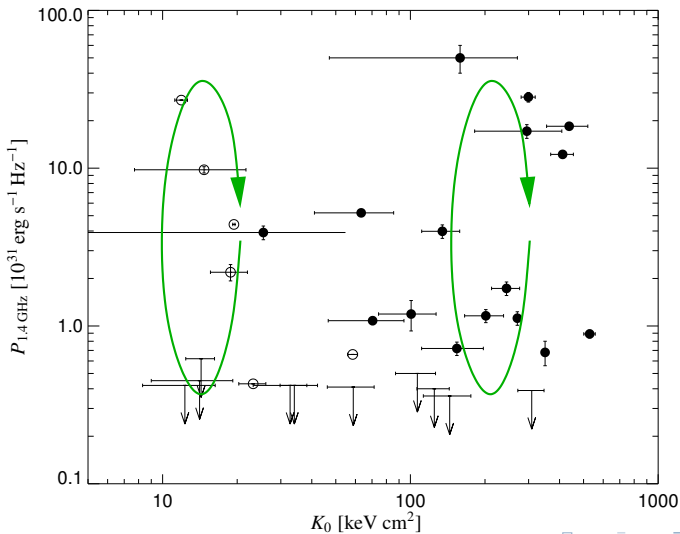
Radio luminosity - central entropy



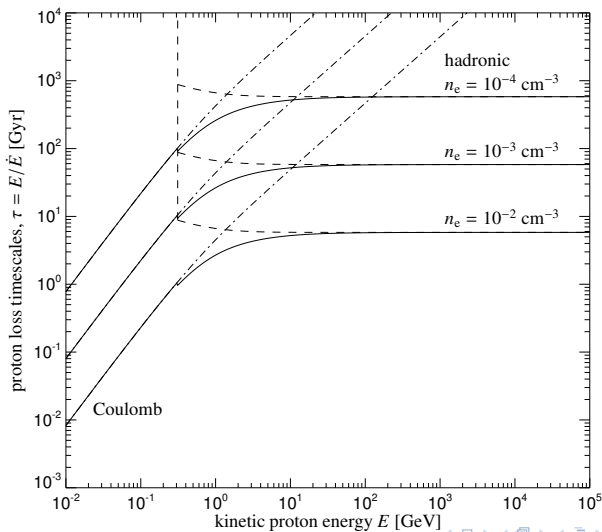
Radio luminosity - central entropy



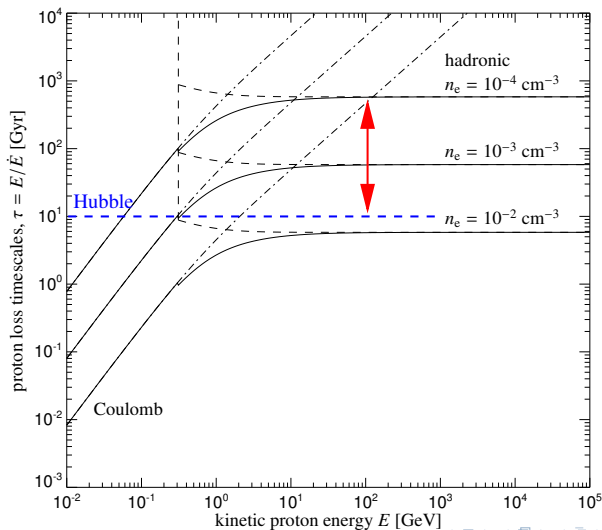
Radio luminosity - central entropy



Proton cooling times



Proton cooling times



Radio halo theory – (ii) re-acceleration model

strength:

- all required ingredients available:
radio galaxies & relics to inject CRe, plasma waves to re-accelerate, ...
- reported complex radio spectra emerge naturally
- clusters without halos ← less turbulent



Radio halo theory – (ii) re-acceleration model

strength:

- all required ingredients available:
radio galaxies & relics to inject CRe, plasma waves to re-accelerate, ...
- reported complex radio spectra emerge naturally
- clusters without halos ← less turbulent

weakness:

- Fermi II acceleration is inefficient – CRe cool rapidly
- observed power-law spectra require fine tuning
- ...



Radio halo theory – (ii) re-acceleration model

strength:

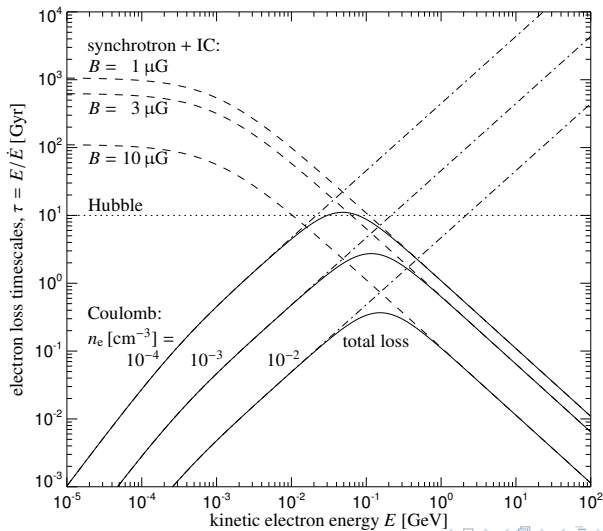
- all required ingredients available:
radio galaxies & relics to inject CRe, plasma waves to re-accelerate, ...
- reported complex radio spectra emerge naturally
- clusters without halos ← less turbulent

weakness:

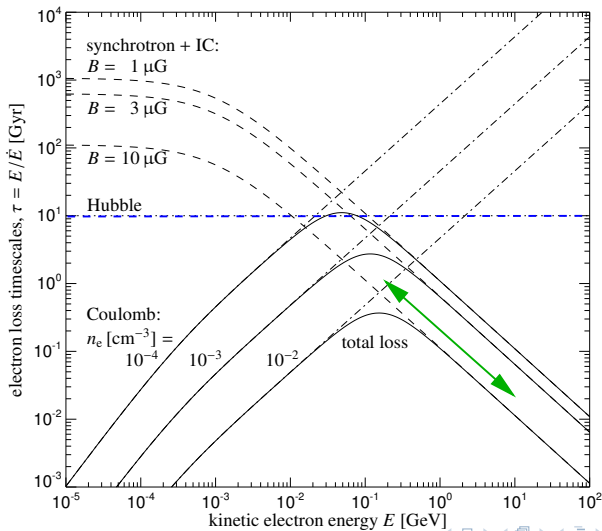
- Fermi II acceleration is inefficient – **CRe cool rapidly**
- observed power-law spectra require fine tuning
- ...



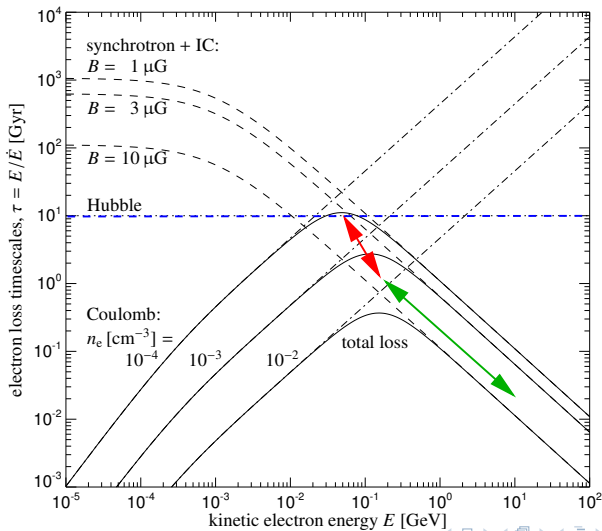
Electron cooling times



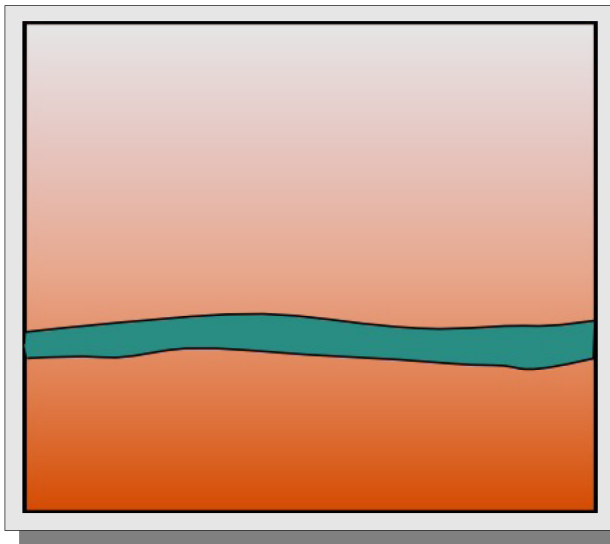
Electron cooling times



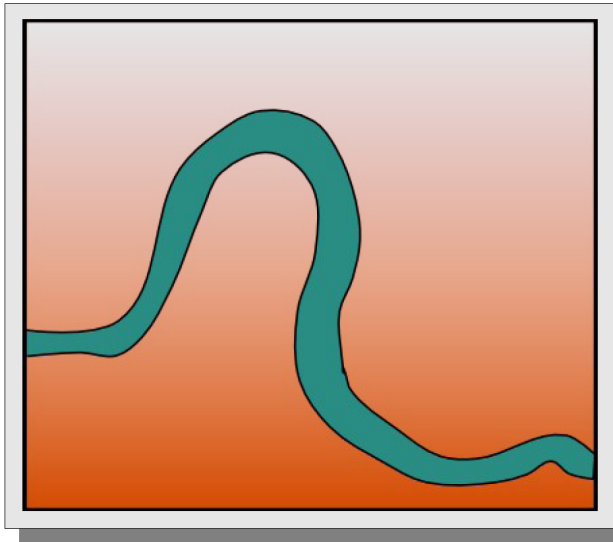
Electron cooling times



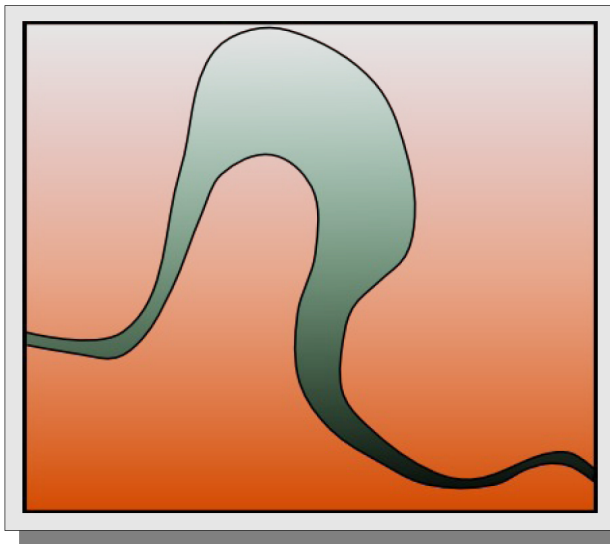
Cosmic ray transport – magnetic flux tube with CRs



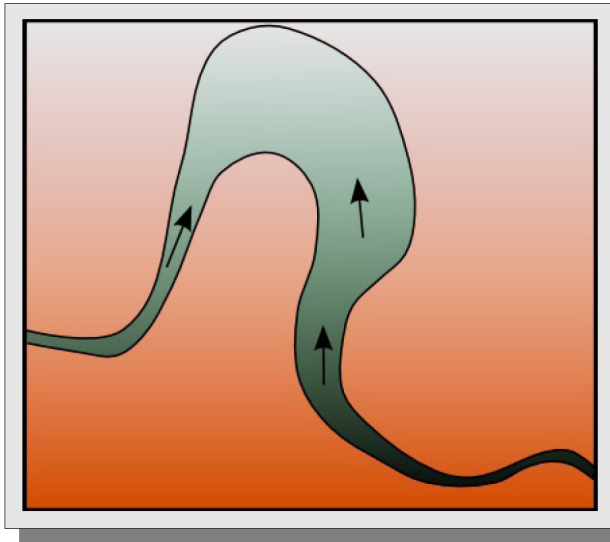
Cosmic ray advection



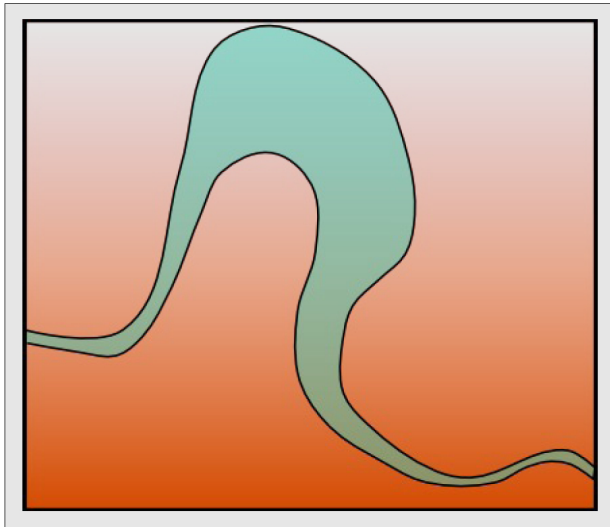
Adiabatic expansion and compression



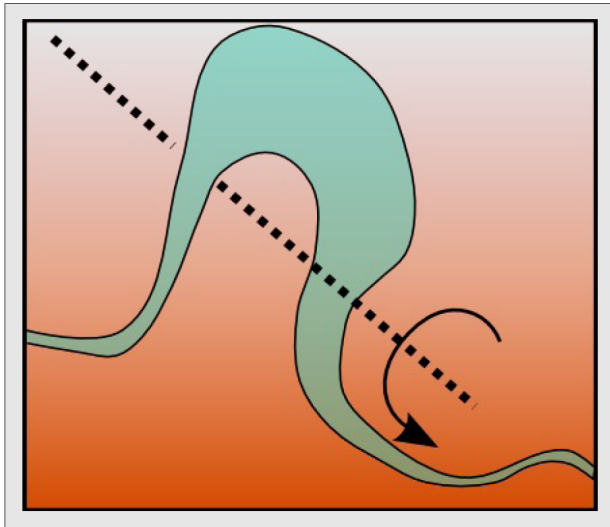
Cosmic ray streaming



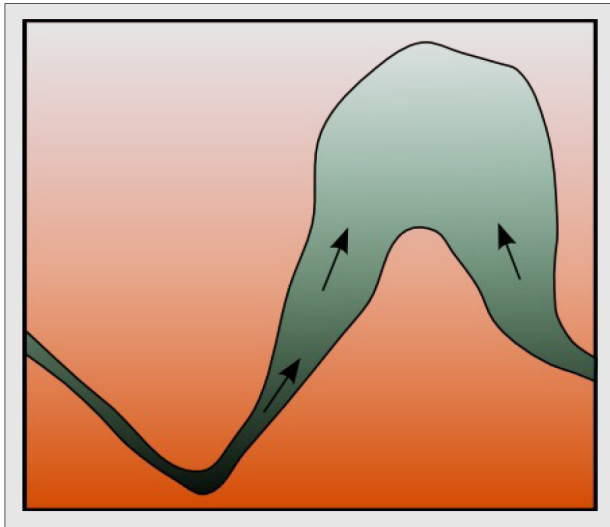
Expanded CRs



Turbulent pumping

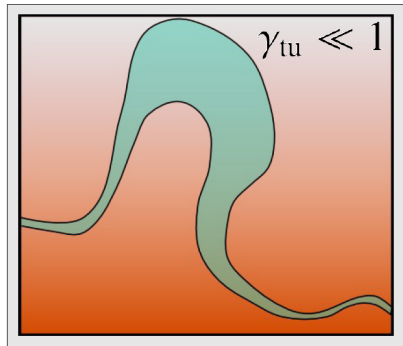
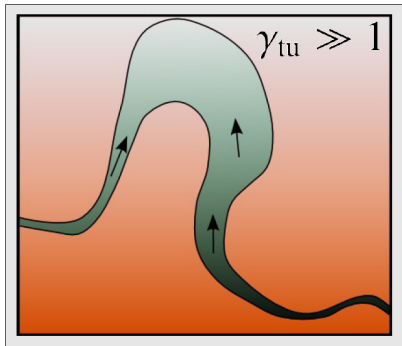


Turbulent pumping

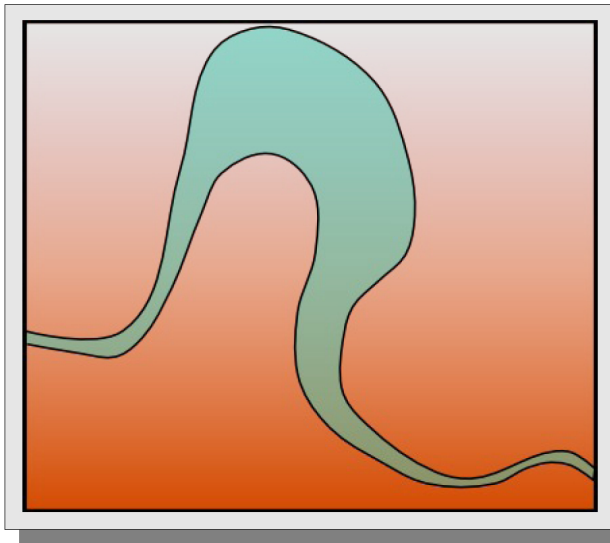


Turbulent-to-streaming ratio

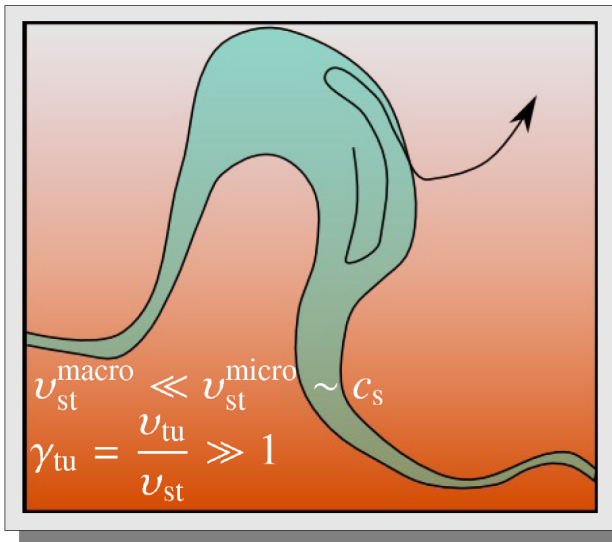
$$\gamma_{tu} = \frac{v_{tu}}{v_{st}}$$



Are CRs confined to magnetic flux tubes?



Escape via diffusion: energy dependence



CR transport theory

CR continuity equation in the absence of sources and sinks:

$$\frac{\partial \rho}{\partial t} + \nabla \cdot (\mathbf{v} \rho) = 0$$

$$\mathbf{v} = \mathbf{v}_{\text{ad}} + \mathbf{v}_{\text{di}} + \mathbf{v}_{\text{st}}$$

$$\mathbf{v}_{\text{st}} = -v_{\text{st}} \frac{\nabla \rho}{|\nabla \rho|}$$

$$\mathbf{v}_{\text{di}} = -\kappa_{\text{di}} \frac{1}{\rho} \nabla \rho$$

$$\mathbf{v}_{\text{ad}} = -\kappa_{\text{tu}} \frac{\eta}{\rho} \nabla \frac{\rho}{\eta}$$

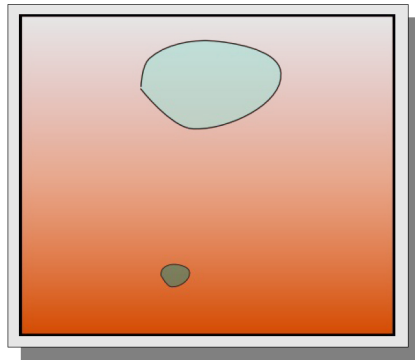
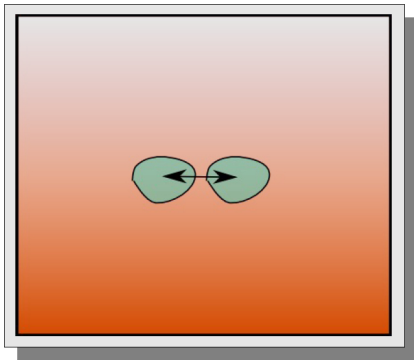
$$\kappa_{\text{tu}} = \frac{L_{\text{tu}} v_{\text{tu}}}{3}$$

Enßlin, Pfrommer, Miniati, Subramanian, 2011, A&A, 527, 99

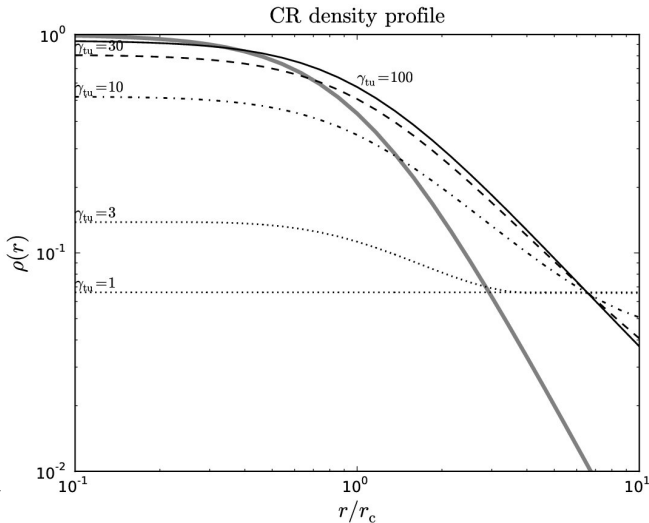


CR profile due to advection

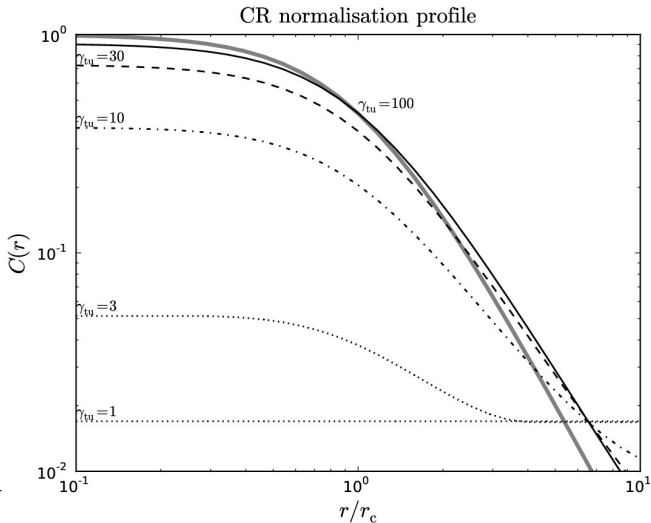
$$\eta(r) = \left(\frac{P(r)}{P_0} \right)^{\frac{3}{5}}$$



CR density profile

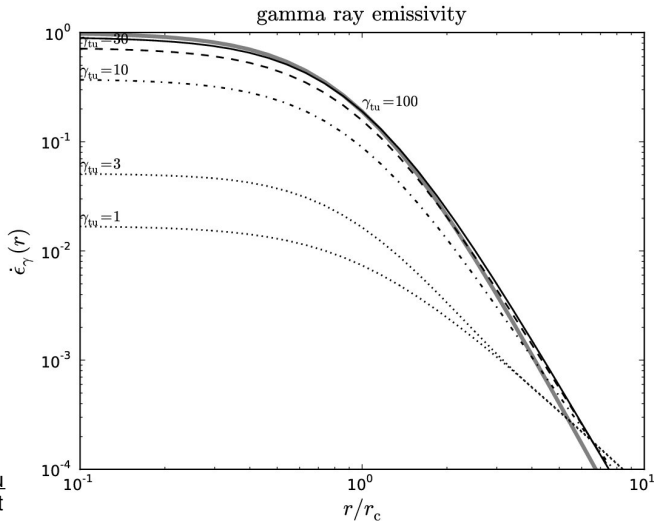


CR density at fixed particle energy



Gamma-ray emission profile

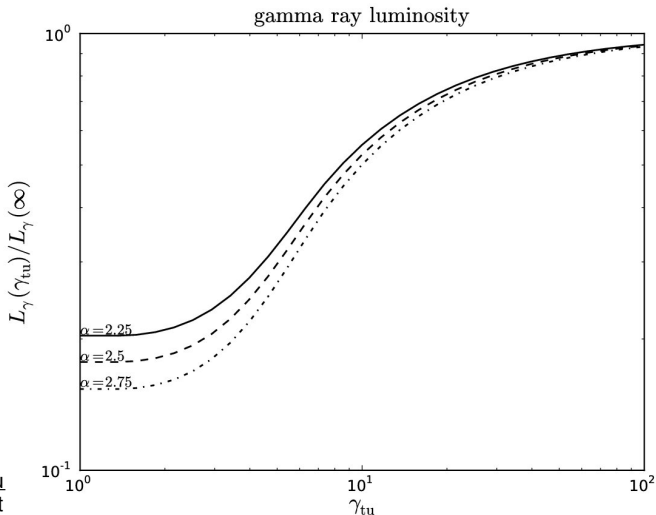
$$p_{\text{CR}} + p \rightarrow \pi^0 \rightarrow 2\gamma$$



$$\gamma_{tu} = \frac{v_{tu}}{v_{st}}$$

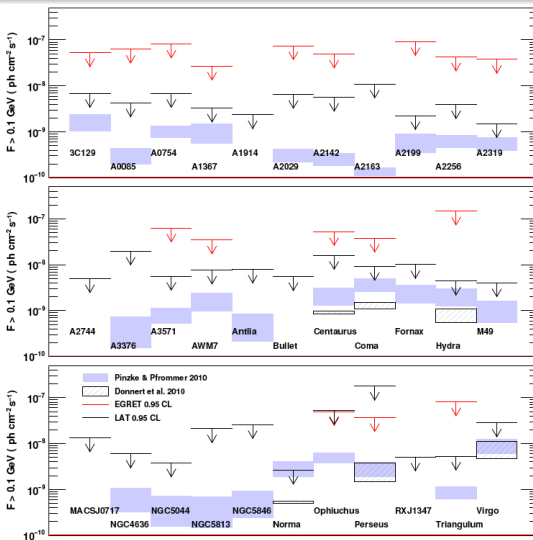
Gamma-ray luminosity

$$p_{\text{CR}} + p \rightarrow \pi^0 \rightarrow 2\gamma$$

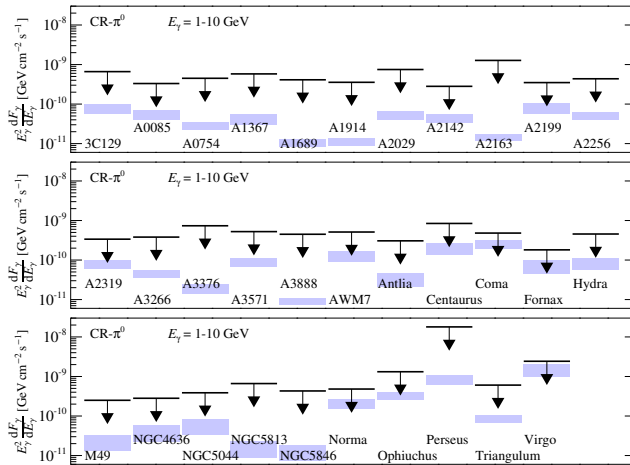


$$\gamma_{\text{tu}} = \frac{v_{\text{tu}}}{v_{\text{st}}}$$

γ -ray limits and hadronic predictions (Ackermann et al. 2010)

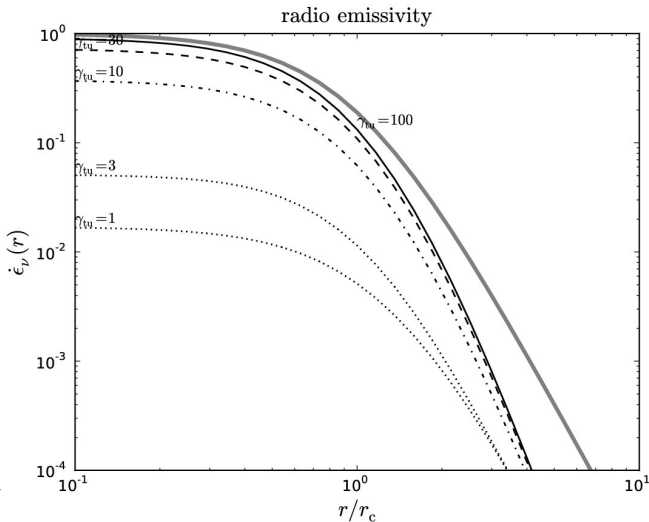


γ -ray limits and hadronic predictions (Pinzke et al. 2011)



Radio emission profile

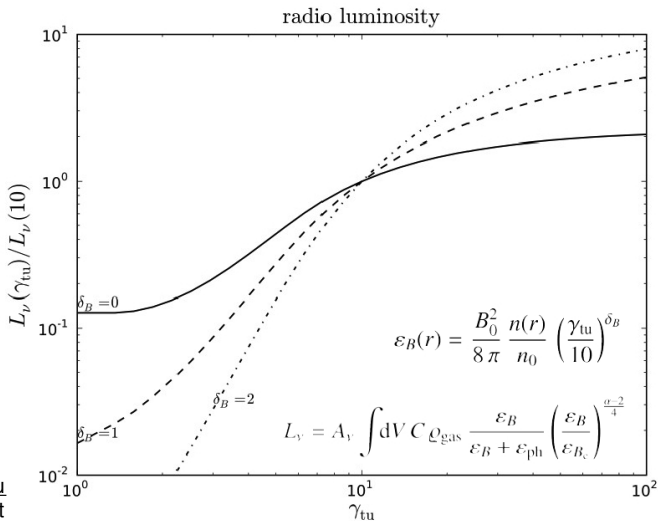
$$p_{\text{CR}} + p \rightarrow \pi^{\pm} \rightarrow e^{\pm} \rightarrow \text{radio}$$



$$\gamma_{tu} = \frac{v_{tu}}{v_{st}}$$

Radio luminosity

$$p_{\text{CR}} + p \rightarrow \pi^\pm \rightarrow e^\pm \rightarrow \text{radio}$$



$$\gamma_{\text{tu}} = \frac{v_{\text{tu}}}{v_{\text{st}}}$$



AIP



Conclusions on radio halos and CR transport

- streaming & diffusion produce spatially flat CR profiles
advection produces centrally enhanced CR profiles
→ profile depends on advection-to-streaming-velocity ratio

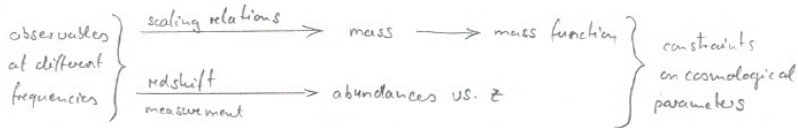
Conclusions on radio halos and CR transport

- streaming & diffusion produce spatially flat CR profiles
advection produces centrally enhanced CR profiles
→ profile depends on advection-to-streaming-velocity ratio
- turbulent velocity \sim sound speed \leftarrow cluster merger
CR streaming velocity \sim Alfvén speed \leftarrow plasma physics
→ peaked/flat CR profiles in merging/relaxed clusters

Conclusions on radio halos and CR transport

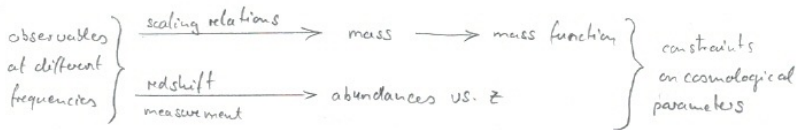
- streaming & diffusion produce spatially flat CR profiles
advection produces centrally enhanced CR profiles
→ profile depends on advection-to-streaming-velocity ratio
 - turbulent velocity \sim sound speed \leftarrow cluster merger
CR streaming velocity \sim Alfvén speed \leftarrow plasma physics
→ peaked/flat CR profiles in merging/relaxed clusters
 - energy dependence of v_{st}^{macro} \rightarrow CR & radio spectral variations
→ outstreaming CR: dying halo \leftarrow decaying turbulence
- bimodality of cluster radio halos & gamma-ray emission!

Cluster cosmology: general picture



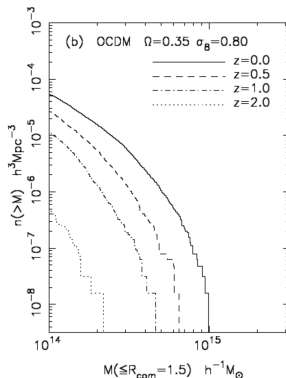
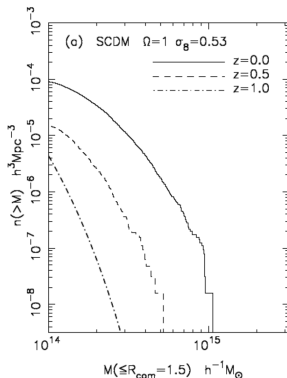
- Cluster abundance to measure the fluctuation amplitude σ_8
- Cluster abundance evolution to measure $\Omega_m = \Omega_c + \Omega_b$
- Cluster baryon fraction to estimate Ω_b/Ω_m
- Cluster distribution to estimate power spectrum and baryon acoustic oscillations in the large-scale structure
- Cluster thermal SZ power spectrum to measure fluctuation amplitude σ_8
- Cluster core structure as a test of the nature of dark matter

Cluster cosmology: general picture



- Cluster abundance to measure the fluctuation amplitude σ_8
problem: converting cluster observables (L , T , ...) to mass
- Cluster abundance evolution to measure $\Omega_m = \Omega_c + \Omega_b$
problem: possible evolution of the L - M or T - M relations
- Cluster baryon fraction to estimate Ω_b/Ω_m
problems: X-rays sensitive to clumping, extrapolation to R_{200}
- Cluster distribution to estimate power spectrum and baryon acoustic oscillations in the large-scale structure
problem: sparse sampling
- Cluster thermal SZ power spectrum to measure fluctuation amplitude σ_8
problem: cluster physics (AGN feedback) affects Compton- y
- Cluster core structure as a test of the nature of dark matter
problem: how does cD assembly affect DM profile?

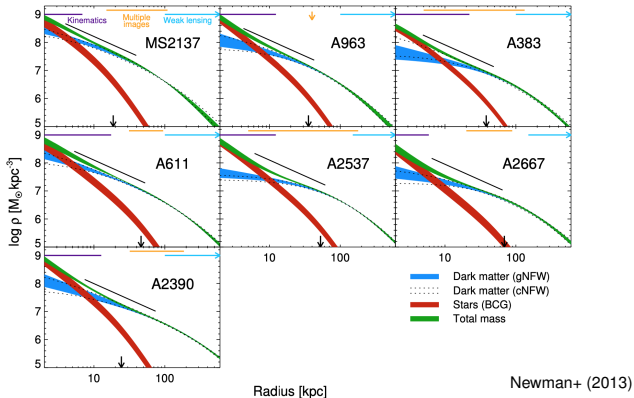
Cluster abundance



Bahcall+ (1997)

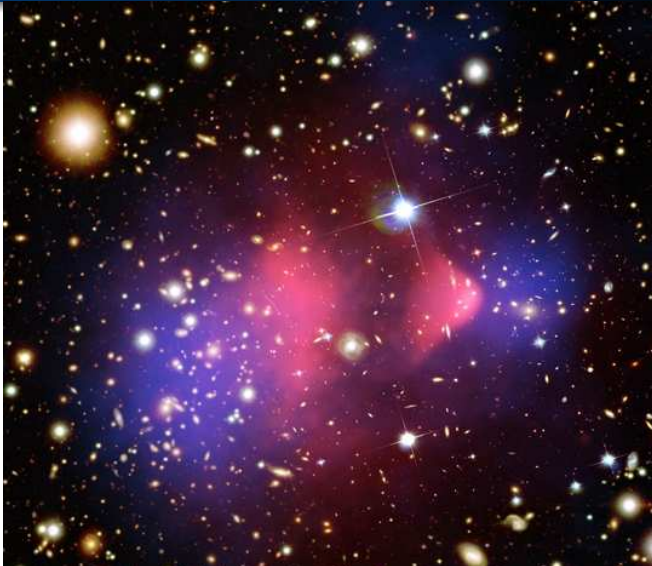
- cluster abundances at a given redshift z are given by a combination of the parameters σ_8 and Ω_m
- cluster evolution sets σ_8 and Ω_m separately so that a measurement of cluster abundances as a function of z breaks degeneracy and constrains σ_8 and Ω_m

Clusters probe the nature of dark matter – 1



- radial density profiles for dark matter halo, stars in the BCG, and their total
- black line segment has slope $\rho \propto r^{-1.13}$ (from DM-only simulations)
 \Rightarrow tension with cold DM or cluster physics modifies density slopes?

Clusters probe the nature of dark matter – 2



AIP



Conclusions

- the non-thermal universe uncovered by high-energy radiation provides **new probes of fundamental physics and cosmology**
- optical and X-ray astronomy have provided impressive discoveries of new phenomena; **now the age of low-frequency and high-sensitivity radio astronomy has begun and cosmic ray physics is about to open up**
- this enables **new insights into the most energetic phenomena in the universe and to study plasma physics and non-equilibrium processes** such as shock acceleration and turbulence
- smart idea for **brilliant minds to join this field of theoretical astrophysics and cosmology** where individuals can make a change instead of participating in (industrially) big collaborations

Conclusions

- the non-thermal universe uncovered by high-energy radiation provides **new probes of fundamental physics and cosmology**
- optical and X-ray astronomy have provided impressive discoveries of new phenomena; **now the age of low-frequency and high-sensitivity radio astronomy has begun and cosmic ray physics is about to open up**
- this enables **new insights into the most energetic phenomena in the universe and to study plasma physics and non-equilibrium processes** such as shock acceleration and turbulence
- smart idea for **brilliant minds to join this field of theoretical astrophysics and cosmology** where individuals can make a change instead of participating in (industrially) big collaborations

→ **non-thermal multi-messenger analyses:**

“The only true voyage of discovery would be not to visit new landscapes but to possess other eyes and to behold the universe through the eyes of another, of a hundred others.”

Marcel Proust



AIP